IBN-KHALDOUN UNIVERSITY OF TIARET
FACULTY OF APPLIED SCIENCES
DEPARTMENT OF ELECTRICAL ENGINEERING

FINAL YEAR PROJECT

For the Master's degree

Domain: Science and Technology

Branch: Electrical engineering

Option: Electrical controls

THEME

Intelligent Control Of A PV Solar System Connected To The Grid In The Case Of Unbalanced Grid Faults

Prepared by: Abdelsamed Ayoub ACHOUR and Nassreddine MOHAMMED

Examination Board

First and last name	Grade	Quality
Said HASSAINE	Pr	President
Ahmed SAFA Hamiche AIT-MIMOUN	MCA MCB	Examiner
Youcef MIHOUB Aicha ASRI	MCA MCB	Supervisor

ACKNOWLEDGEMENTS

Abreviation	Signification
DC	Direct current
FF	Form factor
FLC	Fuzzy Logic Controller.
GPV	Fuzzy Logic Controller
INC	Incremental conductance
MLI	Pulse Width Modulation
MPPT	Maximum Power Point Tracking
P&O	Disrupt and Observe
PV	Photovoltaic
SOC	Battery state of charge.

Symbol	Signification	Unite
E_{ref}	Reference irradiance in nominal condition (1000).	[W/m²]
I_D	Diode current.	[A]
I_L	The current across the Boost inductance.	[A]
I_{cc}	Short-circuit current.	[A]
I_{mpp}	Maximum point current.	[A]
I_{ph}	Photonic current.	[A]
I_{pv}	The current delivered by the PV module.	[A]
I_s	The boost output current.	[A]
I_{sat}	Saturation current.	[A]
k_i	Short-circuit temperature coefficient.	[A/°C]
k_v	Open circuit temperature coefficient.	[V/°C]
P_{max}	Maximum power	[W]
R_s	PV cell series resistance.	[Ω]
R_{sh}	The shunt/parallel resistance of the PV cell.	[Ω]
T_{ref}	Reference temperature in nominal condition.	[K]
V_{co}	Open circuit voltage.	[V]
V	Boost input voltage.	[V]
V_{mpp}	Maximum point voltage.	[V]
V_{pv}	The voltage delivered by the PV module.	[V]
V_S	Boost output voltage.	[V]
f	Converter cut-off frequency.	[Hz]
i_s	DC bus current on generator side	[A]

i_g	Mains-side DC bus current	[A]
C	Continuous bus capacitor capacity	[F]
V_{dc}	DC bus voltage	[V]
L_t	Passive filter inductance	[H]
R_t	Passive filter resistor.	[Ω]
i_{dc}	Continuous bus current.	[A]
P	Active power.	[V]
Q	Reactive power.	[V]
$(u_g)_{dq}$	Network voltages in reference frame (dq)	[V]
V_s	the voltage on the generator side	[V]
E_{max}	Amplitude of Vs.	
I_{max}	The amplitude of the generator current.	
ω_{gr}	The electrical angular velocity of the network.	
P_s	Electrical power supplied by the photovoltaic system.	[W]
ΔI	Current ripple.	[A]
ΔT	Difference between cell temperature and nominal temperature.	[K]
ΔV	Output voltage ripple.	[V]
E	PV module irradiance.	[W/m²]
K	The Boltzmann constant ($1.381.10^{-23}$)	Joule/Kelvin
T	PV module temperature.	[K]
n	The diode ideality factor.	---
q	The electron charge ($1.602.10^{-19} c$).	[C]
α,D	Converter duty cycle [0; 1].	---
η	Energy efficiency.	---

λ	The wavelength.	[m]
I_{charge}	Load current.	[A]
C_{dc}	Central bus capacity.	[F]
TON	Switch running time.	[S]
TOFF	Switch-off time.	[S]
Q1	Superior interepter.	
Q2	Lower interpreter.	
du	The Q1 duty cycle.	
dL	The Q2 duty cycle.	

Chapter I : **Photovoltaic Systems**

Chapter II : **Modeling A Grid-Connected Photovoltaic System**

Chapter III : **Intelligent Control for PV Systems**

Chapter IV : **Simulation.results**

Contents Table

Chapter II : Modeling A Grid-Connected Photovoltaic System

General
Introduction

In the history of humanity, energy is the foundation of all activities. The use of renewable energy sources is very ancient, as they were for a long time the primary means of energy production. The industrial revolution changed this situation. This change was marked in the 19th century with coal and the discovery of steam engines. In the 20th century, the emergence of oil, gas, and nuclear power weakened the use of renewable energies [1].

Today, a large part of the global energy demand is met from fossil resources. Although these fossil fuel reserves are limited, the consumption of these sources leads to greenhouse gas emissions and an increase in pollution. Some developed countries have turned to renewable energies such as solar energy, wind power, biomass, etc.

Solar energy comes from the sun. This star provides tremendous luminous energy to the Earth, which warms the planet and is essential for the survival of many living beings. The problem lies in the fact that the form in which we receive this energy is not necessarily directly usable. That is why we need to use energy conversion processes. Photovoltaic solar cells convert the sun's light energy into electrical energy. Thus, there are areas in the world that are more favorable in terms of solar potential than others. These areas are identified in the form of atlases and highlight "solar deposits" [2].

Adapting the voltage and current levels of the elements of the electrical energy (solar panels, load, batteries, and networks) with respect to a DC bus requires a DC-DC static converter [3]. In a photovoltaic system, the employed DC-DC converters are of the Buck, Boost, and Buck-Boost types. In our study, we focus on the Boost converter.

DC-DC static converters generate a adjusted DC voltage from a fixed DC voltage. The Boost converter acts as a voltage lifter, meaning that the input voltage will be increased thanks to the structure of this converter. It consumes little power and allows a very good efficiency.

Solar panels, although they are becoming more and more efficient, still have relatively low efficiencies (around 20%). That's why it is necessary to extract the maximum power they can generate by minimizing energy losses. An important characteristic of these panels is the maximum available power, which is provided only at a single operating point called the "Maximum Power Point" (MPP), defined by a given voltage and current. This point moves according to weather conditions (sunlight, temperature, etc.) as well as load variations. Extracting the maximum power, therefore, requires a mechanism to track this point called "Maximum Power Point Tracking" (MPPT).

Many MPPT methods have been proposed in the literature, such as the perturb and observe method (P&O), the hill climbing method (HC), and the incremental conductance method (INC). Intelligent control techniques have also been proposed to improve the performance of these methods. In particular, fuzzy logic, artificial neural networks. The choice of this solution is justified by the fact that artificial intelligence allows capturing the operator's know-how and system knowledge without necessarily relying on a mathematical model, which is not always easy to determine. The objective of this work is the application of intelligent control on MPPT, which will act on the duty cycle that will command the Boost converter for photovoltaic conversion.

The presented thesis is organized into:

The first chapter is dedicated to the general presentation of photovoltaic systems. The characteristics and operation of photovoltaic cells will be detailed.

The second chapter presents the modeling of the photovoltaic system and its characteristics. We present the static converter used, namely the Boost converter, through its equivalent circuit and its operation. Subsequently, we move on to its modeling and simulation in open loop.

The third chapter focuses on the presentation of classical MPPT methods such as the P&O method, IC method, and intelligent methods. The two proposed solutions based on fuzzy logic, fuzzy-IC, are presented. To better understand our working method, we will start by presenting the principle of MPPT control and then move on to the proposed intelligent MPPT methods, as well as a reminder of the theory used.

In the final chapter, the development of the model in the MATLAB/Simulink environment is explained. Simulation results are presented, interpreted, and compared for the different strategies

Chapter I:

Photovoltaic Systems

I.1.Introduction

Photovoltaic solar energy comes from the conversion of sunlight into electricity using small cells or photovoltaic cells that are simply placed under the light to generate electric current, without rotating machinery and without noise. The name Photovoltaic comes from the Greek, and is made up of two parts:

Photos: Light.

Volt: Unit of electrical voltage, named after Alessandro Volta.

I.2. History of photovoltaic energy development

The phenomenon was discovered in the 19th century by physicist Alexandre Edmond Becquerel. The first photovoltaic cell was developed in early 1954 for powering satellites. Since 1958, photovoltaic cells have been used exclusively to power satellites, until their first terrestrial applications in the early 1970s. Photovoltaics were used to power small isolated houses and telecommunications equipment [1] .

This chapter introduces the basic concepts of photovoltaics.

History of photovoltaic energy development

Table I 1 Photovoltaic energy History

1839	French physicist Edmond Becquerel discovered the process of using sunlight to produce electric current in a solid material. This is the photovoltaic effect.
1875	Werner Von Siemens presents a paper on the photovoltaic effect in semiconductors to the Berlin Academy of Sciences.
1912	Albert Einstein was the first to explain the photovoltaic effect, and was awarded the Nobel Prize in Physics in 1921 for this explanation.
1954	Three American researchers, Chapin, Pearson and Prince, develop a high-efficiency photovoltaic cell at a time when the fledgling space industry is looking for new solutions to power its satellites.
1958	A cell with an efficiency of 9% is developed. The first satellites powered by solar cells are sent into space.
1973	The first home powered by photovoltaic cells is built at the University of Delaware.
1983	The first photovoltaic-powered car covers a distance of 4,000 km in Australia.
1995	Grid-connected photovoltaic rooftop programs were launched in Japan and Germany, and have been in widespread use since 2001.
At present, worldwide production of solar-generated electricity is around 185.9 TWh [2].	

I.3.Solar radiation

Despite the considerable distance separating the sun from the earth (150.10 6 Km), the earth's surface receives a significant amount of energy (180.10 6 GW), which is why solar energy is such an attractive alternative to other energy sources. This energy leaves its surface in the form of electromagnetic radiation ranging in length from 0.22 to 10 μm [3], the energy associated with this solar radiation breaks down roughly as follows:

9% in the ultraviolet band (< to 0.4μm).

47% in the visible band (0.4 to 0.8 μm).

44 % in the infrared band (> 0.8μm).
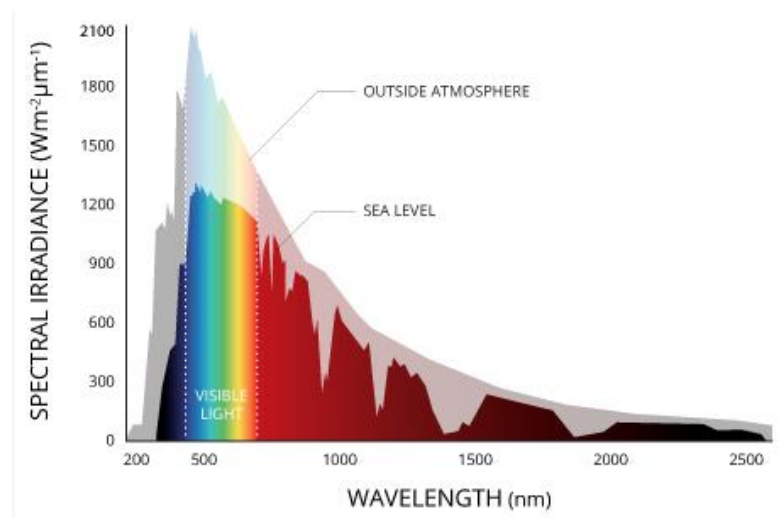
Figure I 1 Spectral analysis of solar radiation.

I.4.Solar energy in Algeria

The study of solar deposits is the starting point for any investigation into solar energy. Solar deposit is a set of data describing the evolution of available solar radiation in a given location and over a given period of time. It can be evaluated using global solar irradiation data. It is used to simulate the likely operation of a solar energy system, and thus to design it as accurately as possible to meet the energy requirements. Algeria's geographical location means that it has one of the highest solar deposits in the world. The average national insolation period exceeds 3,000 hours per year. This figure can easily reach 3,900 hours in the highlands and Sahara. The average daily energy received on a surface inclined to latitude is around 7kWh/m2/day [4]. It is distributed as follows: North: 5.6 kWh/m2/day South: 7.2 kWh/m2/day.Figure (I.2) shows the average annual global irradiation received on an inclined plane at the latitude of the location.
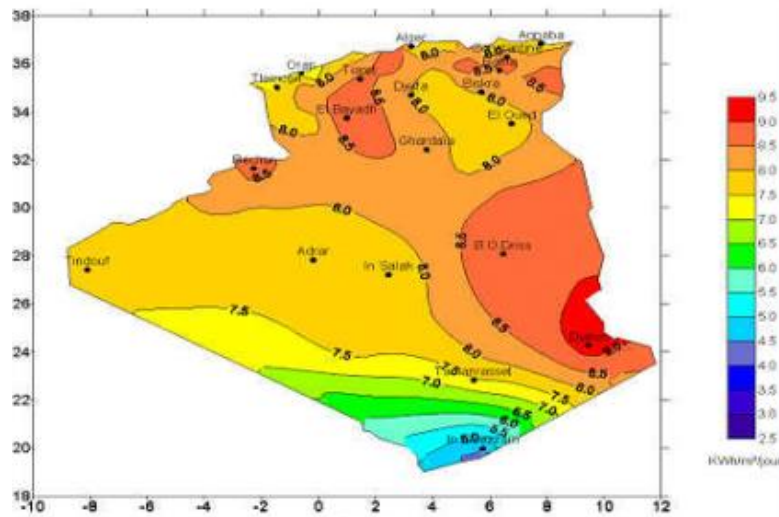
Figure I 2 Global solar irradiation received on a plane inclined to the latitude of the location

I.5.Photovoltaic cells

A photovoltaic cell is an electronic component which, when exposed to light, generates electricity through the photovoltaic effect. The photovoltaic cell is an elementary electrical generator that converts solar energy directly into electricity.

In a photovoltaic cell, the absorption of photons releases negatively-charged electrons and positively-charged "holes". These are collected by an electrode, creating a potential difference between the two terminals. The photovoltaic cell delivers a DC voltage [5].

I.5.1. How it works

A photovoltaic cell is a semiconductor device generally based on silicon. It is made up of two layers, one P-doped and the other N-doped, creating a PN junction with a potential barrier. When photons are absorbed by the semiconductor, they transmit their energy to the atoms of the PN junction, so that the electrons in these atoms are released, creating electrons (N charges) and holes (P charges). This creates a potential difference between the two layers. This potential difference is measurable between the cell's positive and negative terminal connections [6].

I.5.2. The different types of photovoltaic cells

There are several types of cell, depending on the microscopic structure of the silicon:

Monocrystalline silicon cell,

Polycrystalline silicon cells,

Amorphous silicon cell
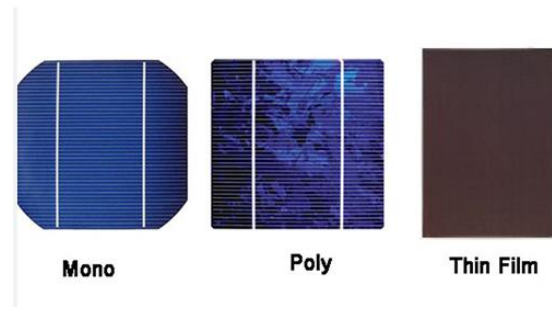
Figure I 3 Type of cells.

I.5.3. Semi-conductor devices

A semiconductor is a material with the electrical characteristics of an insulator. Its advantage lies in the fact that it allows an electric current to pass through it. The electrical conductivity of a semiconductor is said to be intermediate between that of metals and insulators. Above all, these materials are part of the family of electronic components and chips that have become indispensable for driving the latest industrial innovations.

I.5.4. N-type doping

To increase the number of conduction band electrons in intrinsic silicon, pentavalent impurity atoms are added. These are atoms with five valence electrons, phosphorus (P).

In an N-type semiconductor, free electrons are in the majority, while holes are in the minority Figure (I 4).

Donor atoms are pentavalent atoms introduced into the semiconductor to make it extrinsic; these atoms are likely to donate a free electron. This is known as N-type doping.
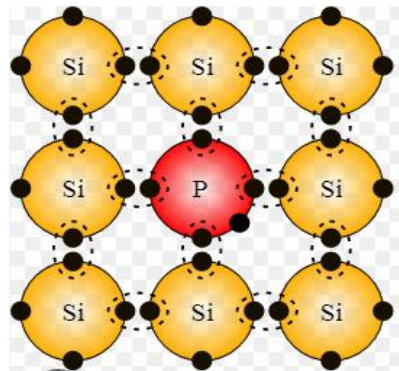
Figure I 4 N-type doping.

I.5.5. P-type doping

To increase the number of holes in intrinsic silicon, trivalent impurity atoms are added. These are atoms with three valence electrons boron (B). The number of holes can be controlled by the amount of trivalent impurity added to the silicon. A hole created by this doping method is not accompanied by a conduction (free) electron. In a P-type semiconductor, holes are in the majority and electrons are in the minority Figure (I 5).

The trivalent atoms introduced into the semiconductor to make it extrinsically P-type are known as acceptor atoms; these atoms are likely to accept a valence electron. This is known as P-type doping.
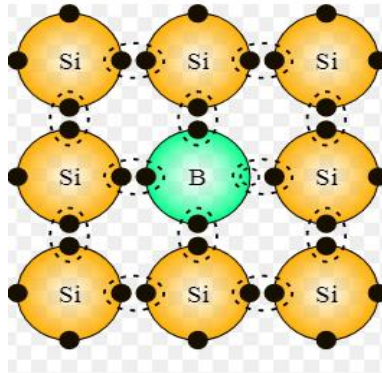
Figure I 5 P-type doping.

I.5.6. PN connection

Each photovoltaic cell consists of a junction called a p-n junction. This means that the top layer of the cell is made of n-type semiconductor and the bottom layer of p-type semiconductor. To obtain this type of junction, the cell surface is treated to deposit the n-type semiconductor on the outer surface of the p-type material.

Once contact has been made, a potential barrier is created. The higher the temperature around this junction, the more the electrons will move and fill all the energy states, thus cancelling the band gap and improving conductivity between the conduction and valence bands.
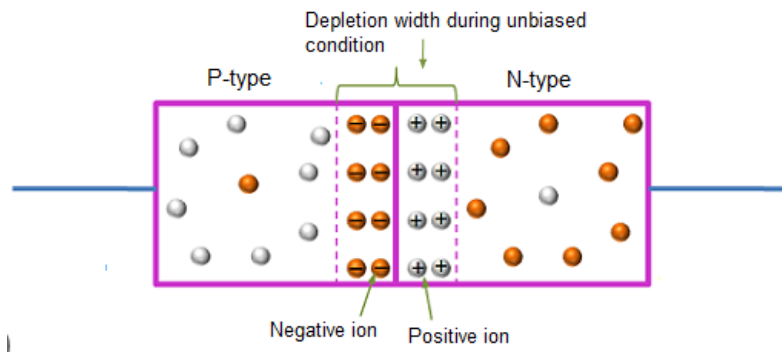
Figure I 6 The operating principle of the p-n junction.

I.6. Advantages and challenges of solar energy

Solar energy is a precious commodity, virtually inexhaustible and promising billions more years of production. So it's in all our interests to take a close interest in it and cherish it! Historically, if we go back far enough, all the energy consumed on Earth comes from the sun, with the exception of nuclear power. Life appeared thanks to the sun, enabling the emergence of animals and plants. Over time, this biomass is transformed into oil and coal. The wind that powers wind turbines is due to temperature and pressure variations, which in turn are due to the sun. Only the uranium used as nuclear fuel is derived from the fusion of lighter atoms in a pre-solar star. We should also be able to

better control the energy the sun sends us. In theory, the amount of energy received by the Earth in one hour would be enough to supply humanity's needs for 1 year if we could harness (and store) it. The major challenges facing solar energy therefore concern its intermittency and storage [7].

I.7Type of photovoltaic system connection

I.7.1. Isolated or stand-alone system

An isolated photovoltaic system supplies the user with electricity without being connected to the grid. It's often the only way to get electricity when grid power isn't available: homes in remote locations, on islands, in the mountains...

This type of system requires the use of batteries for electricity storage and a charge controller to ensure battery durability [8].

I.7.2. Grid-connected system

A grid-connected photovoltaic system is one that is coupled directly to the electricity grid via an inverter. This type of system offers great convenience for the producer/consumer, since the grid is responsible for balancing electricity production and consumption. In the case of grid-connected systems, it is imperative to convert the direct current produced by the photovoltaic system into an alternating current synchronized with the grid. An inverter is used to perform this conversion. Typical inverter efficiency is around 95%. Inverters come in a range of power ratings, and are designed specifically for photovoltaic applications. The inverter also has a grid decoupling function, which prevents current from being injected into the grid when it is not in operation, and an overvoltage protection function [8].

I.7.3. Hybrid system

Hybrid photovoltaic systems integrate a photovoltaic generator with another generator: a wind turbine, a generator set... and sometimes even the public electricity grid. In general, a battery system stores the energy, so you don't lose power from random sources such as solar or wind power. The difficulty with this type of system is to balance the different energy sources in such a way as to optimize all of them, on the understanding that thermal sources (gas, etc.) and the public grid are always the last resort [9].

I.8.General structure of a grid-connected photovoltaic system

There are two types of photovoltaic system structures

I.8.1. PV system connected directly to the grid

The system consists of a photovoltaic generator connected directly to the grid via an inverter.
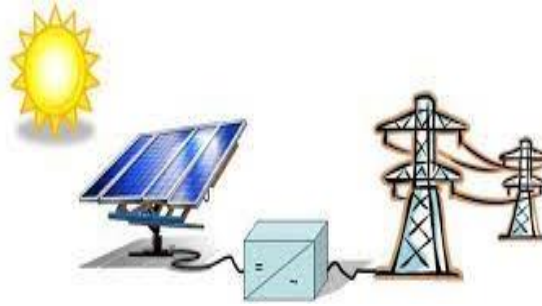
Figure I 7 Photovoltaic system connected directly to the grid

I.8.2. Continuous DC bus systems

The photovoltaic generator is connected via a DC/DC converter. An inverter delivers a modulated voltage, which is filtered to reduce the harmonic content, producing an output voltage that can be fed into the grid.
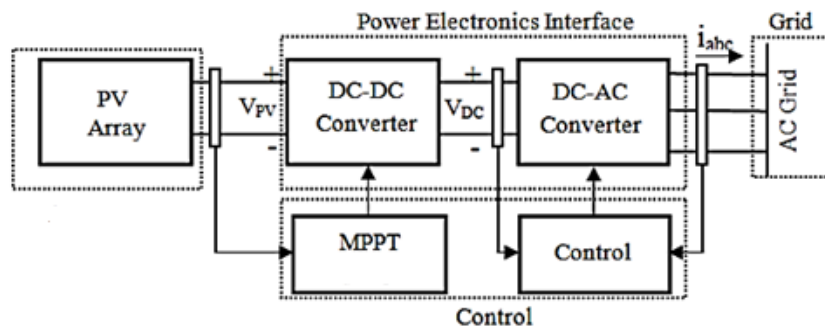
Figure I 8 Photovoltaic system connected via a DC bus.

I.9.Components of a grid-connected system

A grid-connected solar photovoltaic system consists of the following basic components:

- A group of photovoltaic solar panels to convert solar radiation into electrical energy.
- An electrical inverter. The inverter transforms the direct current energy generated by the panels into alternating current.
- An interconnection box for the electrical network.
- An electric meter.

I.10.Coclusion

In conclusion, the first chapter covered the essential points relating to photovoltaic systems, It highlights and emphasizes the significance of photovoltaic systems and also the importance of renewable energy sources in the history of humanity and how the industrial revolution brought about a shift towards non-renewable energy sources.

The chapter underscores the benefits of photovoltaic systems in terms of sustainability, and energy independence. It based on what and how it works their various parts, their architectures and the means of connecting them, we'll move on to modeling the differents parts of the grid-connected photovoltaic system that will be the subject of our study.

Chapter II:

Modeling A Grid-Connected Photovoltaic System.

II.1. Introduction

Modeling is essential for understanding the performance and operation of a grid-connected photovoltaic system. By developing accurate models, we can analyze the behavior of different system components, predict their responses under varying conditions, and optimize system design and control strategies.

One of the key components we'll be focusing on is the DC/DC Boost converter, which is responsible for regulating the flow of energy between the photovoltaic modules and the DC bus. Through modeling, we can understand its voltage conversion characteristics, efficiency and control strategies. This knowledge enables us to ensure efficient extraction of energy from the modules and maintain compatibility with the DC bus voltage.
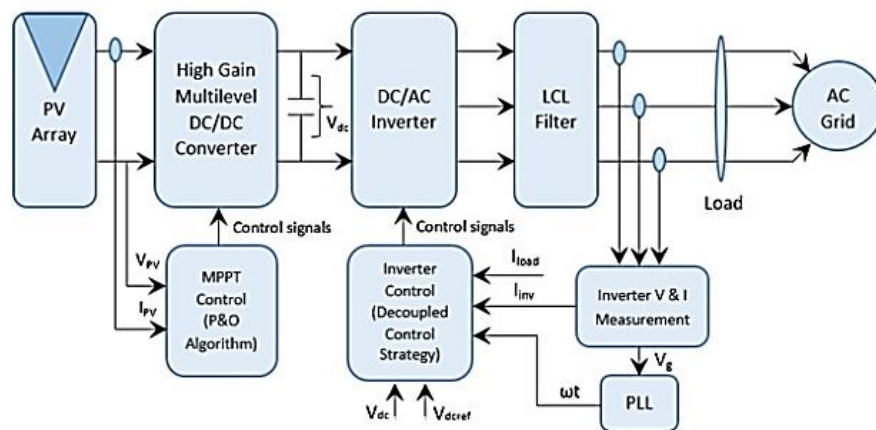
Figure II 1 Diagram of a PV system connected to the grid.

II.2. Photovoltaic cell model

II.2.1 Electrical characteristics of a photovoltaic cell

Figure (II.2) presents the equivalent circuit diagram of a photovoltaic cell under irradiation. It corresponds to a current generator Iph connected in parallel with a diode. Two parasitic resistances are introduced in this diagram, and these resistances have a certain influence on the I-V characteristic of the cell.

The series resistance (R_s): It is the internal resistance of the cell and depends on the resistance of the semiconductor used, the contact resistance of the collecting grids, and the resistivity of these grids.

The shunt resistance (R_{sh}): It is due to leakage current at the junction and depends on how the junction is constructed.

The diode: This diode is in parallel and models the PN junction.
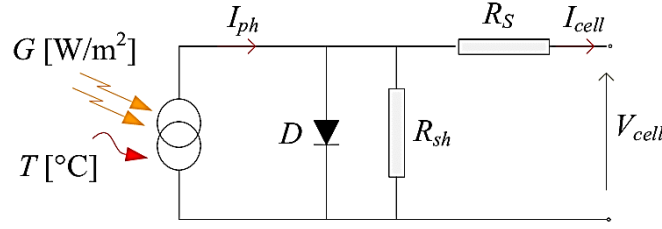
Figure II 2 Circuit of a photovoltaic module.

The mathematical model for the current-voltage characteristic of a PV cell in the simplified equivalent circuit is derived from Kirchhoff's law:

$$I_{pv} = I_{ph} - I_d - I_{sh} \qquad\qquad (II.1)$$

$$I_d = I_{sat}\left(e^{\frac{V_D}{n.V_t}} - 1\right) \qquad\qquad V_t = \frac{K.T}{q} \qquad\qquad (II.2)$$

The relationship is therefore (II.2)

$$I_d = I_{sat}\left(e^{\frac{q(V_{pv}+R_s.I_{pv})}{n.K.T}} - 1\right) \qquad\qquad (II.3)$$

The current in the shunt resistor is calculated by:

$$I_{sh} = \frac{V_{pv} + R_s.I_{pv}}{R_{sh}} \qquad\qquad (II.4)$$

And we deduce the expression for the short supplied by a PV cell:

$$I_{pv} = I_{ph} - I_{sat}\left(e^{\frac{q(V_{pv}+R_s.I_{pv})}{n.K.T}} - 1\right) - \frac{V_{pv} + R_s.I_{pv}}{R_{sh}} \qquad\qquad (II.5)$$

Where:

I_{pv}: is the current supplied by the PV module.

$I_{ph} = I_{cc}(\frac{E}{1000})$: is the photocurrent dependent on the irradiation (E).

Isat: is the saturation current.

K: is Boltzmann's constant (1.381 x 10^(-23) joule/Kelvin).

q: is the charge of an electron (1.602 x 10^(-19) C).

T: is the temperature of the PV module in Kelvin (K).

n: is the ideality factor of the junction (1 < n < 3).

V_{pv}: is the voltage delivered by the PV module.

Rs: is the series resistance representing various contact and connection resistances.

R_{sh}: is the shunt resistance characterizing the junction leakage currents.

II.2.1.1. Short-circuit current

The short-circuit current is the current generated by the cell when the output is short-circuited under irradiation. In other words, when V = 0. For an ideal solar cell, the short-circuit current is equal to the photovoltaic current I_{ph}.

II.2.1.2 Open-circuit voltage Vco

For an ideal solar cell the open circuit voltage is given by:

$$V_{co} = n.V_t.\log(1 + \frac{I_{ph}}{I_{sat}})$$
(II.6)

II.2.1.3 Form factor

The usual operating point of a solar cell is a point on the I(V) curve that corresponds to the maximum power dissipated by the load. The quantity known as the fill factor (FF) is defined as:

$$FF = \frac{P_{max}}{I_{cc}V_{co}} = \frac{I_{mpp}V_{mpp}}{I_{cc}V_{co}}$$
(II.7)

II.2.1.4. Energy performance

The energy efficiency is defined as the ratio of the maximum power supplied by the cell (P_{max}) to the power of the incident solar radiation (P_{in}).

$$\eta = \frac{P_{Max}}{P_i} = \frac{I_{mpp} \cdot V_{mpp}}{\phi.S}$$
(II.8)

Where:

- S: is the surface area of the cell.
- ϕ: is the incident flux.

II.3. GPV modelling

The module involves a current generator to model a diode for the cell's polarization phenomena, a series resistance R_s representing various contact and connection resistances, and a parallel resistance Rsh characterizing the various leakage currents due to the diode and edge effects of the junction.

The photovoltaic generator is represented by a standard single-diode model established by Shockley for a single PV cell, and generalized to a PV module by considering it as a collection of identical cells connected in series-parallel.
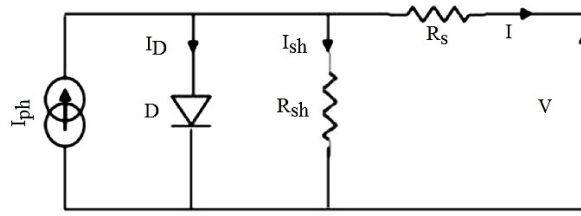
Figure II 3 Equivalent diagram of a photovoltaic cell.

This equivalent circuit consists of a diode (D) representing the junction, a current source I_{ph} representing the photocurrent, a series resistance ($R_{s)}$ representing Joule losses, and a shunt resistance R_{sh} characterizing leakage current between the upper grid and the back current, which is generally much higher than (R_s).

The equation (II.9) characterizing the current of the photovoltaic cell according to the nodal law is:

$$I_{pv} = I_{ph} - I_D - I_{sh} \tag{II.9}$$

Where I_ph is the photocurrent and Id is the current flowing through the diode, and Ish is the current through the shunt resistance.

The expressions for the photocurrent and diode current are given by equations (II.10) and (II.11).:

$$I_{ph} = (I_{cc} + K_i \times \Delta T) \times \frac{E}{E_{ref}} \tag{II.10}$$

$$I_D = I_s \times \left[\exp\left(\frac{V_{pv} + R_s \times I_{pv}}{nV_t}\right) - 1 \right] \tag{II.11}$$

With Is being the saturation current given by the expression:

$$I_s = \frac{I_{cc} + K_i \times \Delta T}{exp\left(\frac{V_{co} + K_v \times \Delta T}{V_{tn}}\right)} \tag{II.12}$$

Where I_{cc} is the short-circuit current, K_I is the short-circuit temperature coefficient, K_v is the open-circuit temperature coefficient, E is the solar irradiance, and E_{ref} is the nominal solar irradiance.

The current through the shunt resistance Ish is presented by the equation:

$$I_{sh} = \frac{V_{pv} + R_s \times I_{pv}}{R_{sh}} \tag{II.13}$$

So, equation (II.1) becomes in the form of the expression:

$$I_{pv} = I_{ph} - I_s \times \left[\exp\left(\frac{V_{pv} + R_s \times I_{pv}}{nV_t}\right) - 1 \right] - \frac{V_{pv} + R_s \times I_{pv}}{R_{sh}} \tag{II.14}$$

Where n is the ideality factor of the diode and Vtest is the thermal voltage.

The equation for the current-voltage characteristic of a photovoltaic generator, with Npp modules in parallel and Nss modules in series, is given by the expression:

$$
\begin{aligned}
I_{pv} = N_{pp}I_{ph} - N_{pp}I_s &\times \left[\exp\left(\frac{V_{pv} + (R_s N_{ss}/N_{pp}) \times I_{pv}}{nV_t}\right) - 1\right] \\
&- \frac{V_{pv+(R_s N_{ss}/N_{pp})I_{pv}}}{R_{sh}N_{ss}/N_{pp}}
\end{aligned}
\tag{II.15}
$$

II.4. GPV characteristics

The figure was shown in the PVG model under the MATLAB environment. It contains blocks of the PV panel equivalent circuit, the result visualization block, and blocks for calculating the currents I_s, I_D, I_{ph}, I_{pv} and I_m.
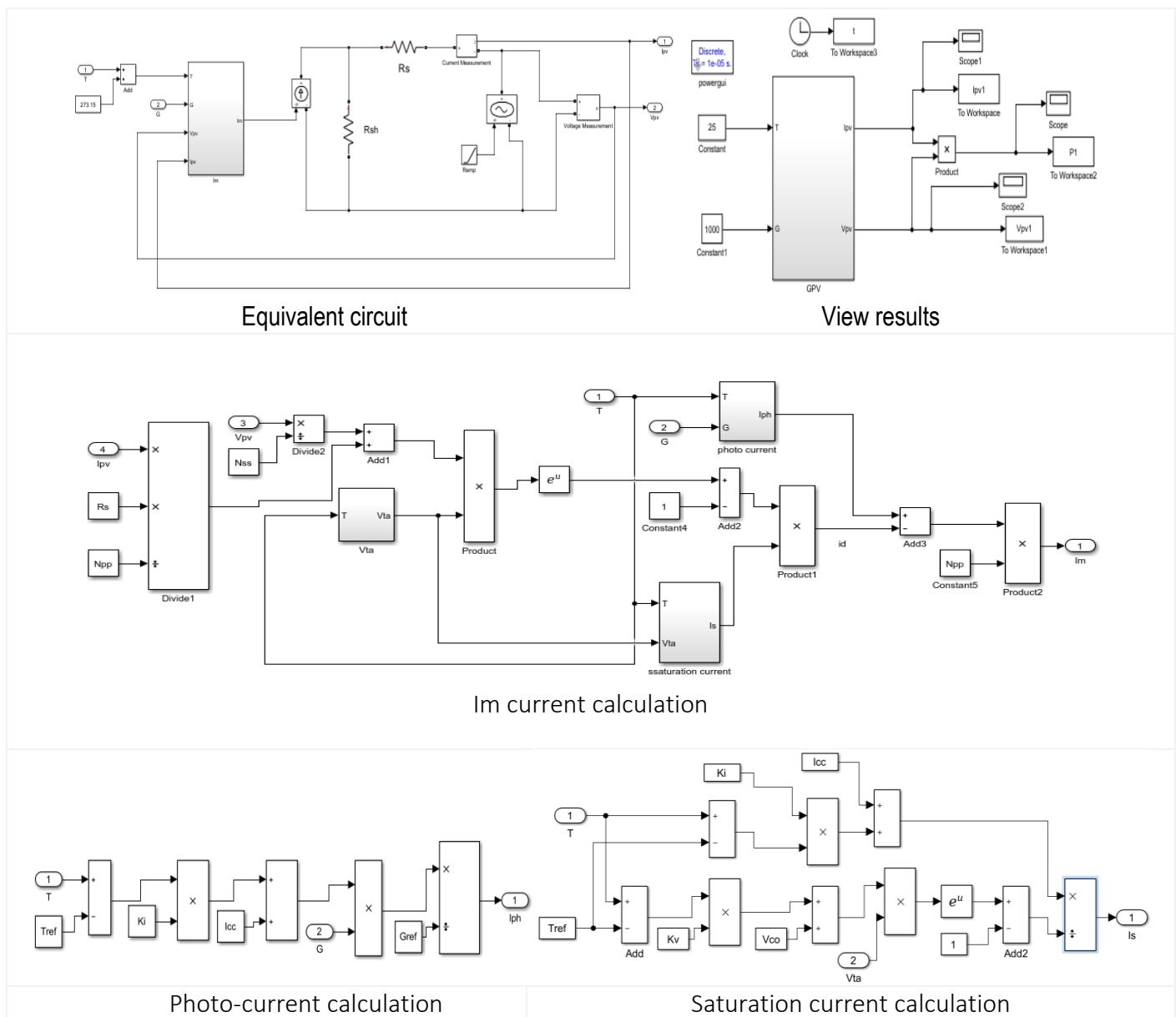
Figure II 4 Block diagram of the improved photovoltaic cell model in Simulink-MATLAB.

II.5. GPV Simulation results

II.5.1 GPV current-voltage-power-voltage characteristics

The result visualization blocks allow for viewing the delivered current, voltage across the photovoltaic generator, as well as its electrical power.

The main characteristics of the solar cell, Ipv=f (V_{pv}) and P=g (V_{pv}), show how a solar cell responds to various possible loads. Generally, the characteristics of our PV cell under standard conditions of 1000 W/m² and 25°C are given by the two figures.
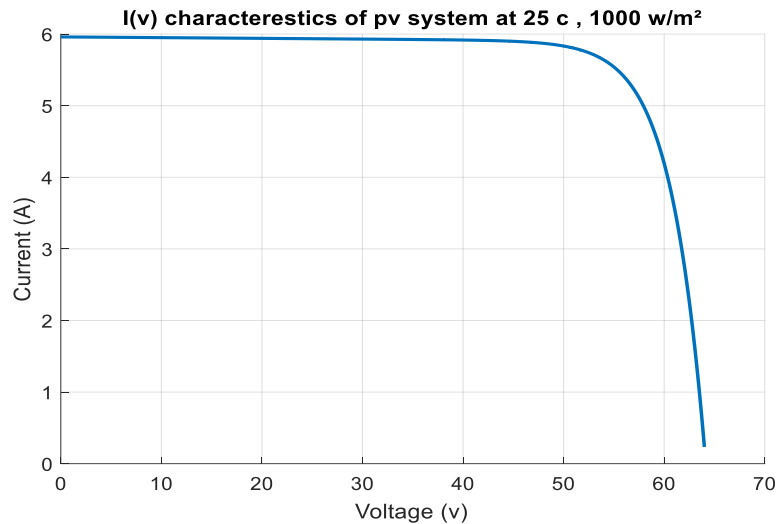
Figure II 5 GPV current-voltage characteristic under standard conditions.
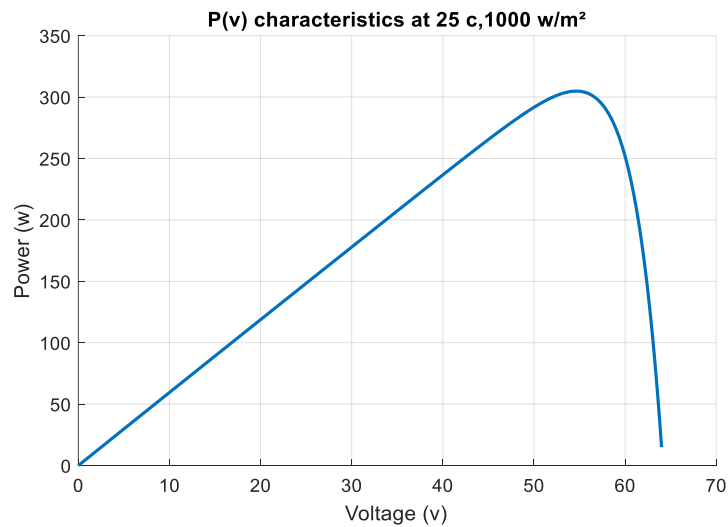
Figure II 6 GPV power-voltage characteristic at standard conditions.

II.5.2. Influence of irradiation levels
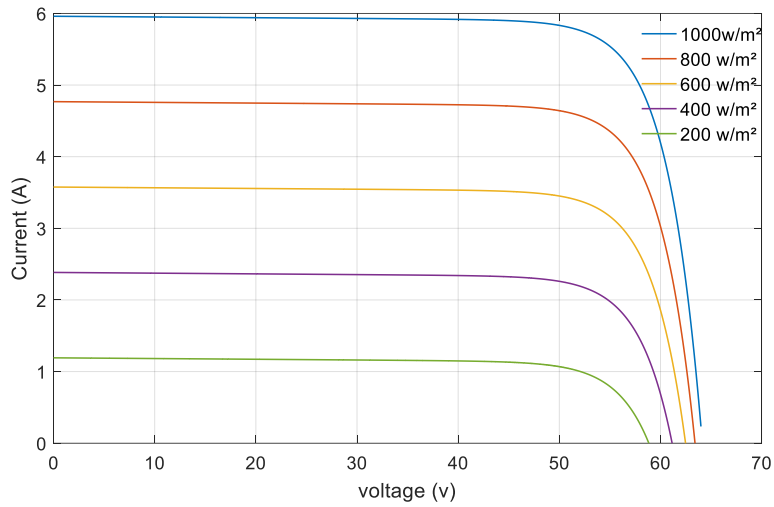
Figure II 7 Influence of irradiation variation on i-v characteristics of GPV for t= 25 °c.

We observe that the short-circuit current value and the irradiaation have the same relationship. However, the open-circuit voltage can vary in different proportions.

We notice the same results regarding the characteristic.$P = g(V_{pv})$
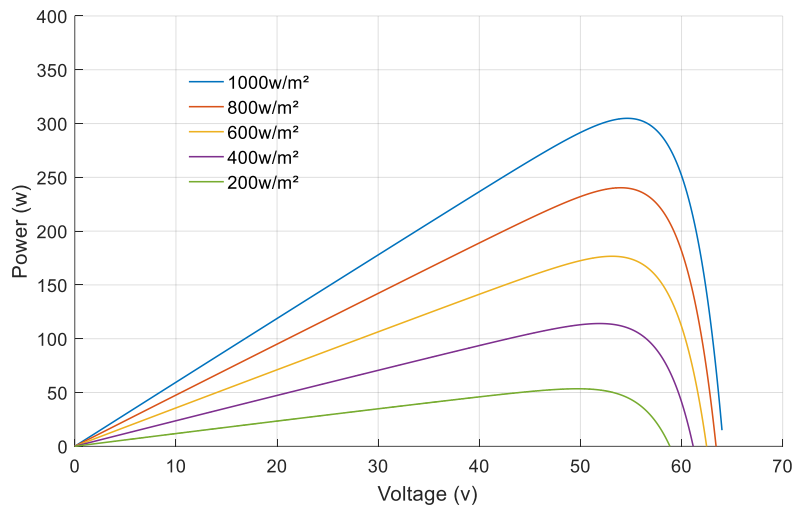
Figure II 8 Influence of irradiation variation on the p-v characteristics of gpv for t= 25 °c.

II.5.3. Influence of temperature

Figures (II 9) and (II 10) illustrate the values of 0, 10, 25, and 50 degrees Celsius of temperature variation under constant temperature conditions.
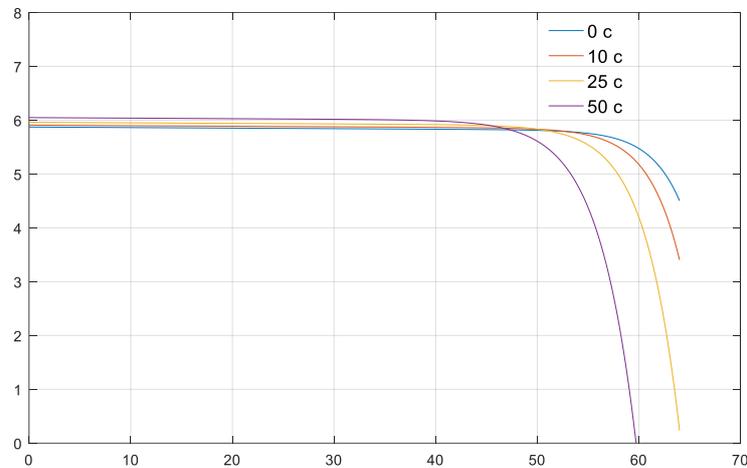
Figure II 9 Influence of temperature variation on GPV's I-V characteristic for E=1000 W/m².
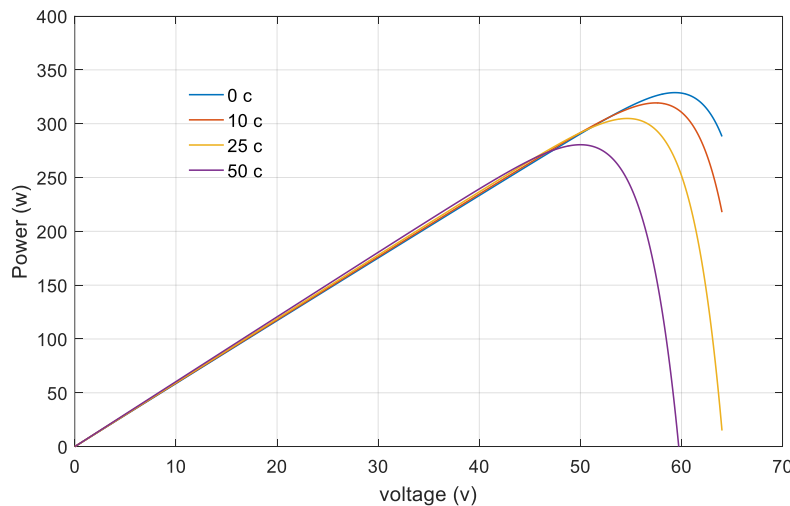
Figure II 10 Influence of temperature variation on the p-v characteristic of gpv for E=1000 w/m².

It can be observed that the value of the short-circuit current is not influenced by the temperature. However, when the temperature increases, the open-circuit voltage decreases significantly, as well as the extractable power.

II.6. DC-DC converters for solar energy

The chopper, also known as a DC-DC converter, is a device used to adapt a continuous energy to a desired voltage level. Its role is crucial as it allows for the storage of photovoltaic energy in batteries and also for supplying a continuous load.

The converter has high efficiency because its components such as capacitors, inductors, and accumulators do not consume active power.

II.6.1. DC-DC converters types

There are two types of converters:

1. Step-up chopper (series, Buck) that allows obtaining an output voltage lower than the input voltage.

2. Step-down chopper (parallel, Boost) that allows obtaining an output voltage higher than the input voltage.

II.6.2. Study of the boost chopper in a PV system

The parallel chopper is also known as a step-up chopper, boost chopper, or Boost-type chopper Figure (II.11). The input source is a DC current source (inductor in series with a voltage source), and the output load is a DC voltage load (capacitor in parallel with the resistive load). The switch "K" can be replaced by a transistor since the current is always positive, and the switching needs to be controlled (during blocking and turning on). The switch can be a MOSFET transistor or an IGBT that can switch between two positions, ON or OFF, rapidly. [10]
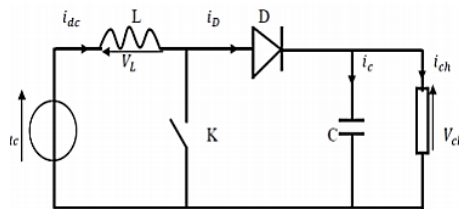
Figure II 11 Electrical diagram of a Boost Circuit

II.6.3. How it works

The controlled switch T is turned on during the period ($0 < t < \alpha T$), and the inductor L is connected to the source, storing a certain amount of energy in the form of current. The diode is in the off state. During the interval ($\alpha T < t < T$), the controlled switch is turned off, and the energy stored in the inductor is released, supplying the load through the diode.
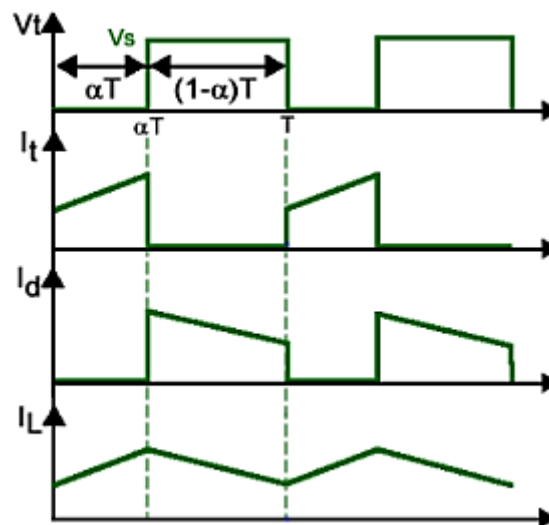
Figure II 12 Wave forms.

II.6.4. Mathematical model of the Boost circuit

When switch K is closed and diode D is open during the interval $(0 < t < \alpha T)$, the electrical circuit of the converter is shown in the figure.
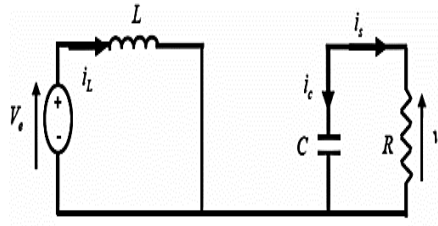
Figure II 13 Equivalent Boost circuit when switch is closed.

$$L\frac{di_L}{dt} = V_e \tag{II.16}$$

$$i_L = I_{min} + \frac{V_e}{L}t \tag{II.17}$$

$$I_{max} = I_{min} + \frac{V_e}{L}\alpha T \tag{II.18}$$

With :

I_{min}: Minimum value of current in the inductor at time t=0.

I_{max}: Maximum value of current in the inductor at time t=αT.

The current ripple in the inductor, $\Delta i_L = I_{max} - I_{min}$, can be calculated using the following equation, which represents the current ripple in the inductor:

$$\Delta i_L = \frac{\alpha V_e}{L}T = \frac{\alpha V_e}{Lf} \tag{II.19}$$

Knowing that:

F: switching frequency.

L: value of the smoothing inductance (H).

Ve: voltage across the generator (V).

T: switching period of the signal of switch T = 1/fp in seconds (s).

α: duty cycle of the switch signal α = t_{on}/T.

i_L: inductor current

When K is open and D is closed during the interval $(\alpha T < t < T)$, the electrical circuit becomes as shown in the figure (II.14).

Figure II 14 Boost equivalent circuit when switch is open.

The equations are as follows:

$$L\frac{di_L}{dt} = V_e - V_s \tag{II.20}$$

$$i_L = I_{max} + \frac{V_e - V_s}{L}(t - \alpha T) \tag{II.21}$$

$$I_{min} = I_{max} + \frac{V_e - V_s}{L}(1 - \alpha)T \tag{II.22}$$

This said, the equality of the two current ripple equations (II.21) and (II.22) gives the mean value of the output voltage Vs:

$$V_s = \frac{1}{1 - \alpha}V_e \tag{II.23}$$

According to the equation, the average output voltage of the converter can be controlled by varying its input voltage or duty cycle. Since the duty cycle is always between 0 and 1, the circuit operates as a voltage booster.

By applying the power conservation principle between the input and output of the converter, we can establish the average value of the current in the inductor in terms of the average current in the load and the duty cycle:

$$I_L = \frac{1}{1 - \alpha}I_s \tag{II.24}$$

During the first operating sequence (0 < t < αT), only the capacitor supplies energy to the load. We can write:

$$c\frac{dv_s}{dt} = -i_s \tag{II.25}$$

Then the output voltage ripple can be expressed as:

$$\Delta V_s = \frac{\alpha i_s}{cf} = \frac{\alpha V_e}{(1 - \alpha)Rcf} \tag{II.26}$$

Regarding the topologies of DC-DC converters, the boost converter is considered the most advantageous in this application due to its simplicity, low cost, and high efficiency. The continuous-continuous step-up converter divides the system voltage into two levels: a variable voltage at the output terminal of the energy source Vi and a fixed DC bus voltage Vdc. The output voltage of the DC bus line of all converters is set to be fixed, and the output voltage of each source is independently controlled

The terminal voltage is adjusted based on both the DC bus voltage and the MPPT controller voltage. Therefore, if an unloaded cell is installed in the network and kept in the same environment as the electricity-generating cells, its open circuit voltage can be periodically measured. By doing so, the operating voltage of the electricity-generating network can be adjusted to match the reference value, which corresponds to the maximum power output. The MPPT technique proposed in this work utilizes a predetermined relationship between the maximum voltage and the open circuit voltage to achieve optimal power point tracking for the PV system under all operating conditions.

The reference rectified voltage values, as well as the DC bus voltage, are sent to a voltage controller. The total power generated by the hybrid system must be controlled to meet the required network and the load demand connected to the network since the PV output power fluctuates with the irradiation. The FC output power is controlled based on the power deficit ΔP, which is the load power (demand value) Ps minus the sum of the power generated from the PV and the battery power Pbat, respectively.

$$Pbat = \Delta P = Ppv - Pcharge \tag{II.27}$$

The constant voltage of the DC bus must be ensured regardless of the load behavior and the value of the power extracted from the PV source. The batteries provide regulation of the DC bus voltage, even in the face of weather changes. At any given time, the sum of the currents, Ibat, Ipv, and ich, must be equal to Idc

$$Pbat = \Delta P = Ppv - Pcharge \tag{II.28}$$

Ibat, Ipv, and icharge correspond to the currents flowing through the DC bus, battery, PV panels, and loads, respectively

$$Cdc \frac{dVdc}{dt} = Ibat + Ipv - Icharge \tag{II.29}$$

The capacity of the central bus Cdc, ensures a common DC bus voltage for both the load and other power sources.

To regulate the DC voltage, a PI controller is utilized.

Acting as an interface between the various power sources and the DC bus, a PWM-based DC/DC power converter is employed. This converter enables control over the energy transfer between the sources, allowing for the regulation of the intermediate circuit voltage (Vdc) by charging or discharging the battery based on the system's requirements

II.7. Mathematical model of the Buck-Boost converter

A bidirectional DC/DC converter (buck-boost converter). Consequently, the current and power flow is bidirectional, depending on the operating conditions (variation in sunlight and load).

The block diagram of the battery's buck-boost DC/DC converter is illustrated in Figure (II.15). It consists of a high-frequency inductor, an output filtering capacitor, and two IGBT switches with diodes [11].

The upper and lower switches serve the purpose of charging and discharging the battery storage system.

The switches Q1 and Q2 are controlled to ensure the converter operates in steady state, divided into four distinct sub-intervals. Here is a brief explanation of the operation during these four time intervals.
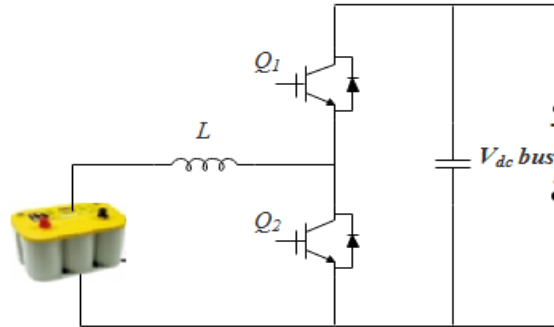
Figure II.15 Schematic block of the Buck-Boost converter.

Interval 1 (to - t1)

In this interval, the lower switch *Q2* is ON and the upper switch *Q1* is OFF with diode *D1* and *D2* reverse biased as shown in Figure (II.16(a)). During this time, the converter operates

In boost mode and the inductor is charged and current through the inductor increases. The battery voltage (*Vbat*) and the increased inductor current ($\Delta ibat$ (+)) are expressed as follows:

$$Vbat = L\frac{dibat}{dt} = L\frac{\Delta ibat}{\Delta T} \tag{II.30}$$

$$\Delta ibat(+) = \frac{Vbat}{L}Ton \tag{II.31}$$

Where *Ton* is the ON time of lower switch *Q2*.

Intervalle 2 (t1 – t2)

In this interval, both switches Q1 and Q2 are in the OFF state. The diode D1 connected to the upper switch Q1 conducts, as depicted in Figure (II.16 (b)). As a result, the current in the inductor begins to decrease. The decrease in inductor current ($\Delta ibat$ (-)) during the OFF state can be calculated using the following equation:

$$\Delta ibat(-) = \frac{(Vdc - Vbat)}{L}TOFF = \frac{(Vdc - Vbat)}{L}(T - TON) \tag{II.32}$$

Where $TOFF$ is the OFF time of lower switch $Q2$ and T is the total time of operation.

During steady-state operation, it is required that the change in inductor current (Δibat (+)) during the ON time and the change in inductor current (Δibat (-)) during the OFF time are equal. Therefore, equation (II.31) and equation (II.32) are equated as follows

$$\frac{Vbat}{L}TON = \frac{(Vdc - Vbat)}{L}(T - TON)$$

(II.33)

The relationship between battery voltage (V_{bat}) and DC link voltage *(V_{dc})* as a function of duty ratio can be expressed as:

$$Vbat = du * Vdc$$

(II.34)

Where du is the duty cycle of the upper switch of the battery converter

Interval 3 (t₂ – t₃)

During the time interval (t2 - t3), the upper switch Q1 is turned ON, and the lower switch Q2 is turned OFF, causing diodes D1 and D2 to be reverse biased, as depicted in Figure (II.16 (c)). In this interval, the converter operates in buck mode. The expression for the inductor current is given by:

$$\Delta ibat(+) = \frac{(Vdc - Vbat)}{L}TON$$

(II.35)

Intervalle 4 (t₃ – t₄)

During this interval*,* both upper switch Q_1 and lower switch Q_2 are turned OFF and the diode D_2 of the lower switch conducts as shown in Figure (II.16 (d)).During this interval, the converter works as a buck converter. The inductor current decreases and expressed as follows:

$$\Delta ibat(-) = \frac{Vbat}{L}TOFF = \frac{Vbat}{L}(T - TON)$$

(II.36)

In steady state operation, Δi_{bat} (+) during ON time and Δi_{bat} (-) during OFF time have to be equal. As a result, (II.35) and (II.36) are equated as follows:

$$\frac{(Vdc - Vbat)}{L}TON = \frac{Vbat}{L}(T - TON)$$

(II.37)

From equation (II.36), the output voltage can be expressed as a function of duty ratio as:

$$Vdc = \frac{1}{1 - dL}Vbat$$

(II.38)

Where d_L is the duty ratio for the lower switch of the battery converter.
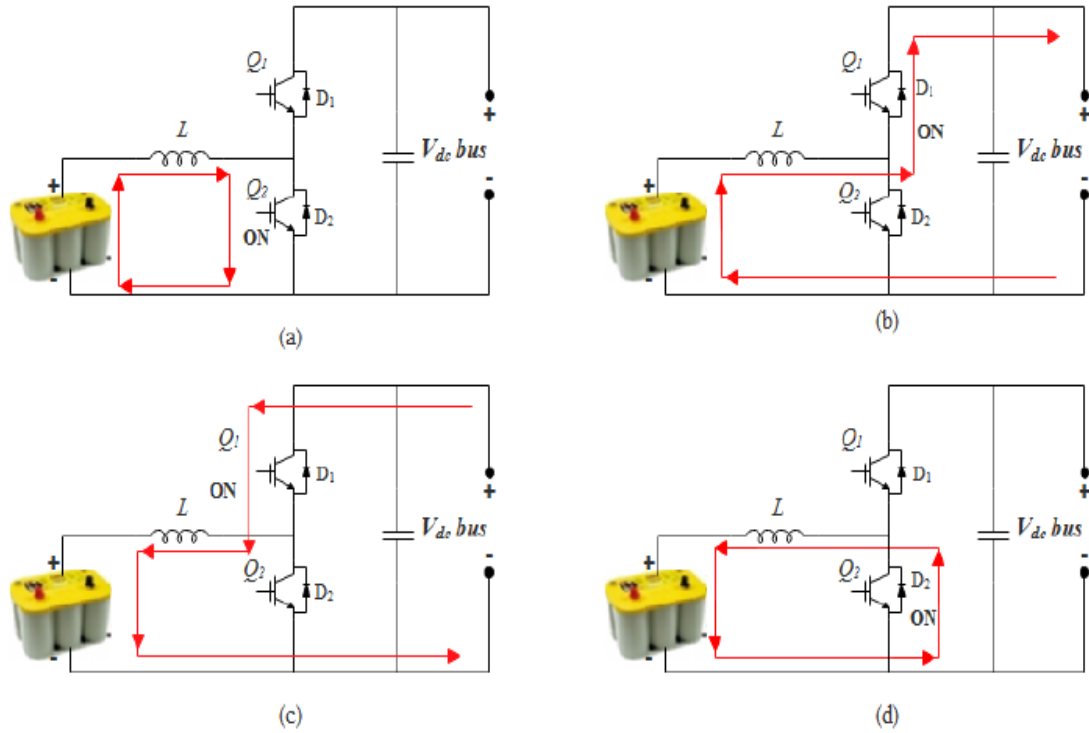
Figure II.16 Buck-Boost converter operation, (a) interval 1, (b) interval 2, (c) interval 2, (d) interval 4.

II.8. Simulation of BOOST circuit

To verify the function of the BOOST converter, which is voltage boosting, we perform simulations using MATLAB.

With :Ve=100V, L=0.00175H, R=15, C=0.0022, α=50%
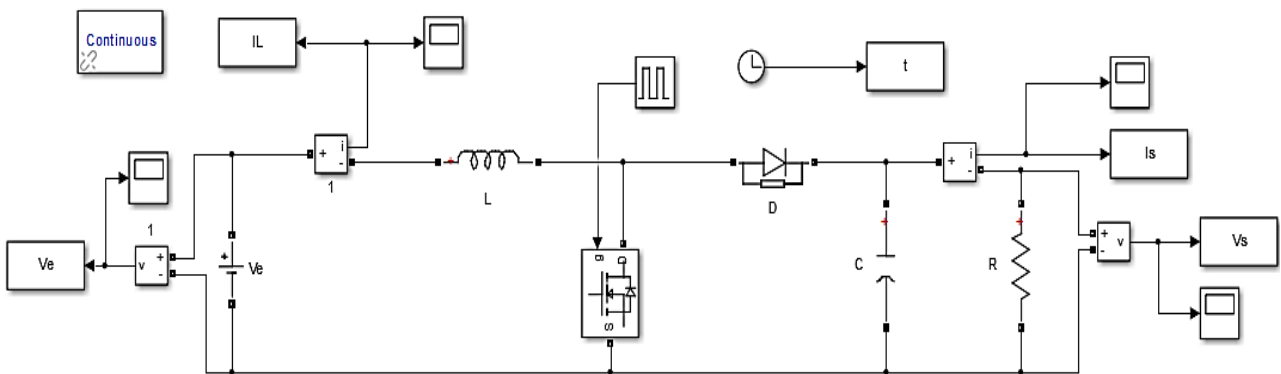
Figure II 15 Simulink block diagram of the boost chopper.
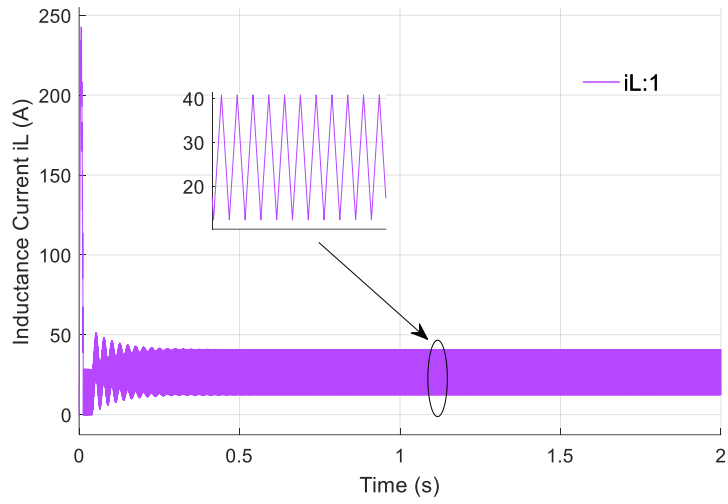
Figure II 16 Inductance current IL
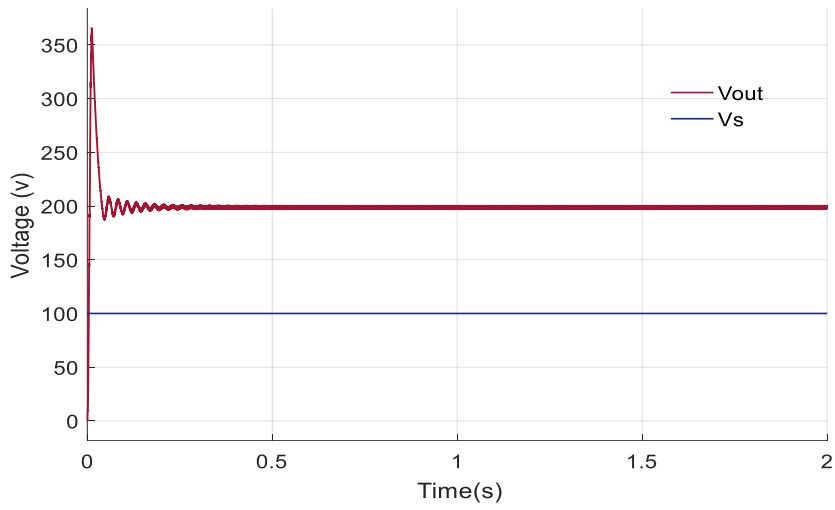
Figure II 17 Boost input and output voltage.
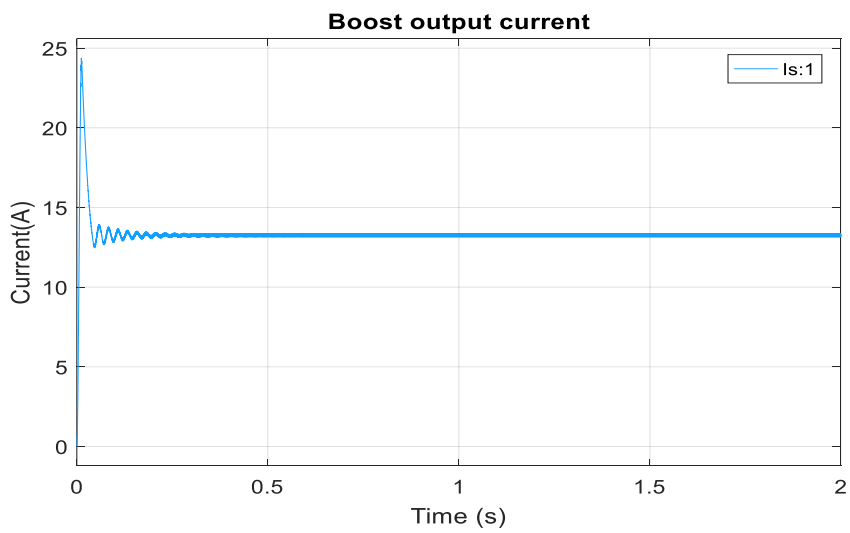
Figure II 18 Boost output current.

II.9. Inverter For PV Systems

An inverter is a power electronics device that converts a direct current (DC) electrical energy source, such as a photovoltaic source, into alternating current (AC) voltages and currents. It is the inverse function of a rectifier. An inverter is a static converter of the DC/AC type [12].

Most inverters are bridge structures, typically composed of electronic switches such as Insulated Gate Bipolar Transistors (IGBTs). The choice of this type of component is based on its ability to switch very high values of current and voltage at switching frequencies of several tens of kHz, and because it allows for the elimination of all the commutation aid circuits required in thyristor-based systems. Two types of inverters are commonly used to achieve such conversion:

- Single-phase inverter.

- Three-phase inverter.

II.10. Checking the mains connection

II.10.1. Mains-side converter control

The Pulse Width Modulation (PWM) converter and the transformer are the tools through which the entire power generation system is connected to the three-phase grid. The constant DC bus voltage must be maintained by the converter regardless of the magnitude and direction of power.

A synchronized reference frame is used to achieve vector control of currents based on the measurement of the DC bus voltage. The references are imposed on the individual phase voltages.

II.10.2. Vdc continuous bus control

The DC bus is the capacitor located between the two converters; its function is to maintain a stable DC voltage. The model of the DC bus is expressed as:

$$C \frac{dVdc}{dt} = i_s - i_g \tag{II.39}$$

Where is is the current of the DC bus on the generator side and ig is the current of the DC bus on the grid side, C being the capacitance of the DC bus capacitor. Assuming the converters are ideal (no power losses), the voltage across the capacitor is expressed as follows:

$$C \frac{dVdc}{dt} = \frac{P_s}{V_{dc}} - i_g \tag{II.40}$$

Where Ps is the electrical power supplied by the photovoltaic system. It can be expressed as follows:

$$P_s = 3V_s i_s = V_{dc} i_{dc} \tag{II.41}$$

Or else:

$$P_s = \frac{3}{2}E_{max}I_{max} = V_{dc}i_{dc} \qquad\qquad \text{(II.42)}$$

Where Vs is the voltage on the generator side and Emax is its amplitude, Imax is the amplitude of the generator current, and i_dc is the current through the capacitor.
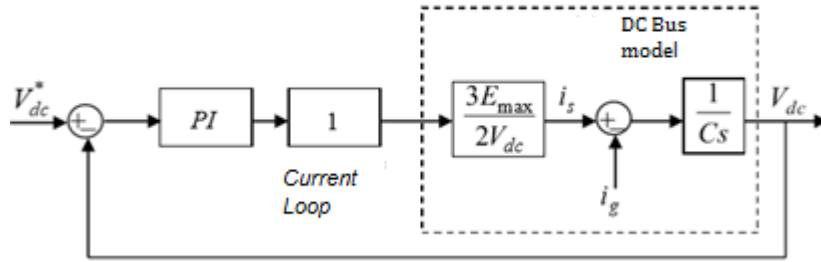
Figure II 19 Vdc loop control diagram.

In this control loop, the current loop is considered to be faster than the voltage loop. We assume it to be equal to 1. The PI controller is designed using the pole placement method.

II.10.3. Active and reactive power control

The dynamic model of grid connection in the synchronously rotating reference frame with the grid voltage space vector is given by:

$$u_{gd} = R_t i_{gd} - \frac{L_t di_{gd}}{dt} + w_{gr}L_t i_{gq} + e_{gd} \qquad\qquad \text{(II.43)}$$

$$u_{gq} = R_t i_{gq} - \frac{L_t di_{gq}}{dt} + w_{gr}L_t i_{gd} \qquad\qquad \text{(II.44)}$$

Where Rt and Lt are the resistance and inductance of the filter, which is located between the converter and the grid. ugd and ugq are the components of the inverter voltage, and ωgr is the electrical angular frequency of the grid.

If the reference frame is aligned with the supply voltage, the grid voltage vector is given by:

$$u=u_{gd} + j0 \qquad\qquad \text{(II.45)}$$

The active and reactive powers delivered to the grid through the converter can be expressed as follow is:

$$\text{P}=\frac{3}{2}u_{gd}i_{gd} \qquad\qquad \text{(II.46)}$$

$$\text{Q}=\frac{3}{2}u_{gd}i_{gq} \qquad\qquad \text{(II.47)}$$

II.11. Battery Energy Storage System

Energy storage provides an opportunity to grasp and balance the PV system as it is produced. It may be stored and used later when the demand is expected to increase the capacity of solor energy production. The research work in this project considers the as an energy storage, and its good performances. The system is clean and functioning. The battery performs reliably and robust over a. One of the main factors for its popularity choice and dominant position is its low cost with good performance and cycle life [11].
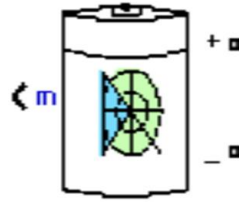
Figure II 20 Battery electrical circuit.

II.11.1 Battery dimensioning

In order to simulate the system, a model of battery has to be defined. In the literature, battery models developed for the sizing and the scheduling are simple with a few parameters such as battery current, capacity, state of charge and temperature. All these parameters are varied with the operating conditions and affected the capacity of battery to charge or discharge [13]. The battery used in this work is modeled by the battery model included in SimPower Systems. It is modeled as a variable voltage source in series with anequivalent internal resistance as shown in Figure (II 21).

As Figure (II 21) illustrates, the battery voltage is given by the following equation:

$$V_{bat} = E_{bat} - R_I . I_{bat}$$ (II.48)

Where *Vbat* is the battery rated voltage, *Ri* is internal resistance (Ω). The battery output voltage *Ebat* for the period of the charging or discharging mode depends on the internal battery parameters such as: the battery current *ibat*, the hysteresis phenomenon during the charging and discharging cycles and the capacity extracted
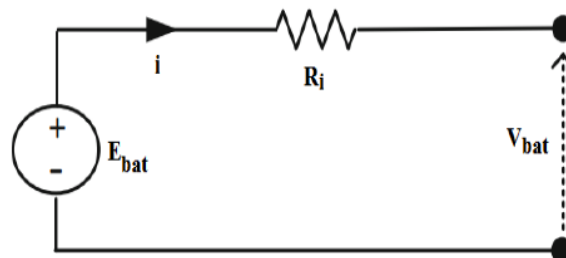
Figure II 21 Simplified a battery model.

II.11.2 Instant characteristics

The state of charge (SOC) of the battery is the parameter related to the number of charges stored in the battery. A SOC of 100% means that the battery is fully charged, whereas at 0% it is considered empty. In real life situations, it is important to maintain the SOC within limits recommended to prevent internal damage, SOC$_{min}$ ≤ SOC ≤ SOC$_{max}$. The SOC is calculated by

$$SOC = 1 - \frac{Q_e}{C(0.\theta)}$$ (II.49)

Another variable widely used in the literature is the depth of discharge (DOD), which describes the emptiness of battery (complement of the SOC). It is defined as:

$$DOC = 1 - \frac{Q_e}{C(I_{avg}.\theta)}$$ (II.50)

Where Q_e (A s) is the battery's charge, DOC is battery depth of charge, I_{avg} (A) is the mean discharge current, and C(A s) is the BES capacity

Discharging mode

In discharge mode where $i_{bat} > 0$, the lead-acid battery is modeled by equation (II.51):

$$E_{bat} = E_0 - K\frac{Q}{Q - i_t}i*_{bat} - K\frac{Q}{Q - i_t}i_t + f_{hyst_{dish}}(i)$$ (II.51)

Charging mode

In charge mode where $i_{bat*} < 0$, the lead-acid battery is modeled by equation (II.52):

$$E_{bat} = E_0 - K\frac{Q}{0.1Q - |i_t|}i*_{bat} - K\frac{Q}{Q - i_t} + f_{hyst_{char}}(i)$$ (II.52)

II.12. The System Control

A hybrid system gestion refers to the management or control of a hybrid system. A hybrid system typically refers to a system that combines different technologies, components, or sources of power to achieve a specific goal or function.

In the context of energy systems, a hybrid system gestion involves the management of a power system that incorporates multiple energy sources, such as renewable energy sources (e.g., solar, wind) and conventional sources (e.g., fossil fuels), along with energy storage and grid infrastructure. The goal of hybrid system gestion is to optimize the operation and utilization of the various components of the system to achieve reliable, efficient, and cost-effective energy generation and distribution.

Key aspects of hybrid system gestion include:

- Resource management: It means when the system must effectively manage the various energy sources, such as prioritizing the use of renewable sources when they are available and optimizing the dispatch of different sources to meet the demand.

- Energy storage management In general hybrid systems often incorporate energy storage technologies, such as batteries, to store excess energy for use during periods of high demand or when renewable sources are not available. Gestion involves managing the charging, discharging, and overall operation of energy storage systems.

- Control and optimization: Gestion entail the application of control algorithms and optimization strategies to effectively coordinate the operation of diverse system components, including power generation, energy storage, and grid integration. The aim is to achieve the highest possible performance and efficiency for the overall system.

- Grid integration and balancing: Hybrid systems are typically connected to the electrical grid. Gestion involves ensuring seamless integration with the grid, managing power flows, and maintaining grid stability by balancing the supply and demand of electricity.

- Monitoring and maintenance: Effective gestion requires continuous monitoring of system performance and maintenance of the various components to ensure optimal operation, identify issues or faults as it is in our case, and carry out necessary repairs for example proposing intelligent controls (ANN) or replacements.

Overall, hybrid system gestion aims to achieve a balance between different energy sources, optimize system performance, and facilitate the transition to a more sustainable and resilient energy infrastructure.the figure explain more
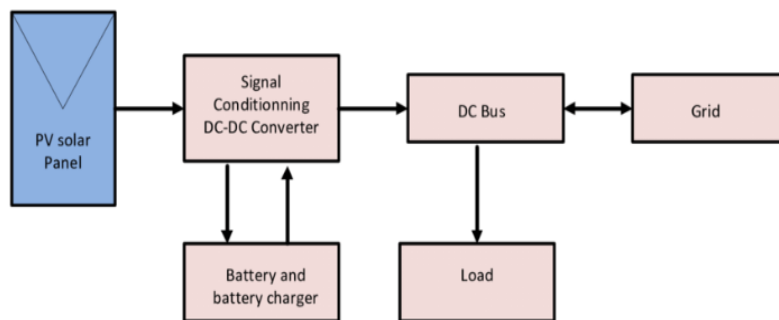
Figure II 22 Simplified a battery model.

II.12. Conclusion

In this chapter, we presented the modeling of a photovoltaic system, starting with the photovoltaic generator by observing the characteristics of the photovoltaic generator (GPV) and its performance under the influence of atmospheric parameters such as temperature and irradiation. Then, we detailed the model of the Boost converter as it is the same for Buck-Boost converter, which represents the adaptation stage between the PV generator and the load.

Also modelling a PV system with storage energy that demonstrated the significant benefits of integrating storage technology. The inclusion of energy storage increases the system's performance by enabling the capture and utilization of excess energy, ensuring a stable power supply even during periods of low solar irradiance.and tempratur This illustrated the system's effectiveness in load management, and grid support.

For the MPPT and the ANN control part, we will provide a more in-depth presentation of this type of control in the next chapter

Chapter III:

Intelligent Control for PV Systems.

III.1 Introduction

The low effeciency of a PV system represent a great disadvantage, so there are some methods that it used to improve its efficiency Therefore, maximum power point tracking (MPPT) controller is required to improve the effeciency of the PV system. A variety of MPPT methods have been developed and improved continuously. These methods include perturb and observe (P&O), Incremental Conductance (IC), Hill Climbing (HC), fractional open-circuit voltage, fractional shortcircuit current, neural network, fuzzy logicmethods, and genetic algorithms. These techniques differ in many aspects such as required sensors, complexity, cost, and range of effectiveness, oscillation around the MPP, convergence speed, correct tracking when irradiation and/or temperature change and hardware implementation [12].

III.2. The MPPT Control

The Maximum Power Point Tracking (MPPT) is essential in the operation of the PV arrays to improve the overall system effeciency. The solar irradiation (E) and the cell temperature (T) are considered to represent the environmental conditions change along the day hours. As E and T vary, the PV array voltage and power depart from the optimum point. Consequently, the PV array voltage is adjusted to match the maximum output power. The common way to adjust the PV voltage is via adjusting the duty cycle of the DC-DC boost converter. The most widespread MPPT methods are the incremental conductance (INC), the perturb-and-observe, and the hill climbing. Driven by the advancements in artifcial intelligence techniques. There are many variants are applied as a controle methods to the PV system [12]. For PV modules, there is one single operating point from where maximum power can be drawn. This point is required to be located or tracked and we need to make sure that functional position of PV module is always at or around this maximum power point. The various MPPT techniques are being established and realized. These techniques differ over-complication, required sensors, implementation charges, tracking time, effective operating range, hardware implementation, acceptance, and reverences. The coming sections present the assessment of several MPPT techniques available and their relative advantages and disadvantages.
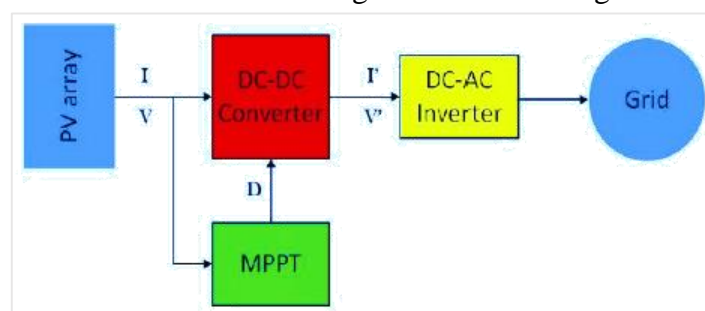
Figure III 1 MPPT control schematic.

III.3. Classical MPPT Methods

III.3.1. Conventional Perturb & Observe Method (P&O)

At present, photovoltaic (PV) has received much interest as a secondary energy source. Due to nonlinear characteristics and low efficiency of photovoltaic arrays, tracking the maximum power point (MPP) of a photovoltaic array is an essential part of a PV system. The

Perturbation and observation is one of the most commonly used MPPT methods for its simplicity and ease of implementation. In this method, the array voltage is slightly disturbed (increase or decrease) then the actual value of the power P(k) is compared to the previous obtained value P(k-1). If the power panel is increased due to the disturbance, It disturbs the operating point of the system, causing the PV voltage to fluctuate near the MPP voltage.. The flowchart of the Perturbation and observation method is illustrated in Figure. (III 2) [12].
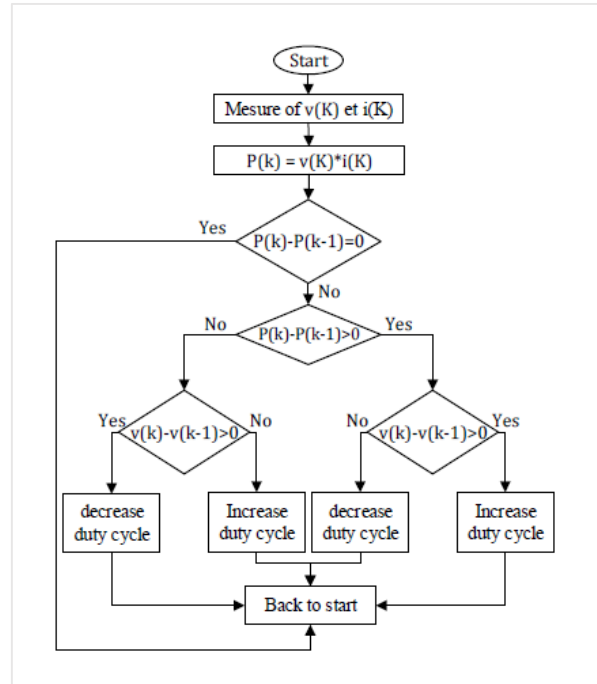
Figure III 2 P&O Algorithm Flowchart.

The P&O algorithm is represented in that way:

- If dpv/dVpv>0 the voltage is increased, this induces an increase in the duty cycle D(K)=D (K-1)+C. C is an accretion constant.

- If dpv/dVpv<0 the voltage is reduced, this results in a decrease in the duty cycle D(K)=D (K-1)-C.

Another drawback of the P&O method is that, as the MPP is reached, the power tracked by the P&O method will oscillate and perturb up and down near the MPP as the module terminal voltage is perturbed for every MPPT cycle resulting in a loss of PV power especially in cases of constant or slowly varying atmospheric conditions. The magnitude of the oscillations is determined by the degree of variations of the output voltage or duty cycle
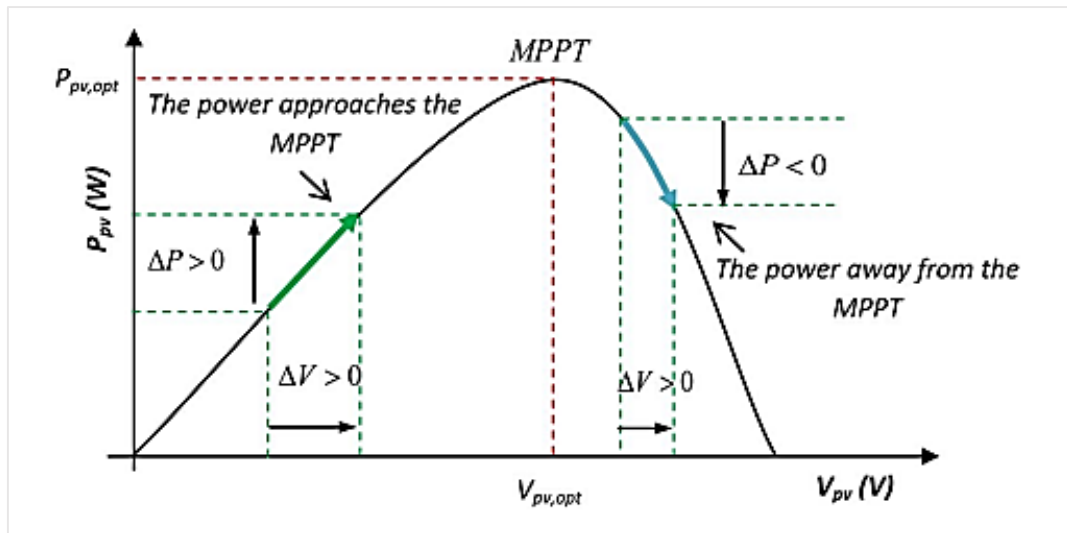
Figure III 3 How MPPT Algorithm work.

III.3.2. Incrémental Conductance Method

The incremental conductance method is one of the widely used conventional MPPT methods. It is based on the slope of the power-voltage relation. which represents the optimal operation point (maximum output power) when reaching zero., whereas negative slope requires voltage decrement and positive slope requires voltage increment to maintain the PV array voltage and power at their optimum values. This algorithm uses the instantaneous conductance I/V and theincremental conductance dI/Dv as it shown in this equations:

$$dI/dV = - I/V \qquad (dP/dV = 0). \text{ At MPP} \ldots \ldots \ldots \ldots \text{ (III.1)}$$

$$dI/dV > - I/V \qquad (dP/dV > 0). \text{ At the left of MPP} \ldots .(III.2)$$

$$dI/dV < - I/V \qquad (dP/dV < 0) \text{ At the right of MPP } .(III.3)$$

The perturbation in the voltage is applied until "(III.1)" is achieved. And the direction of perturbation can be determined by equation "(III.2)" and "(III.3)". A floowchart of the incremental conductance method for MPPT is shown in Figure. For the conventional INC method, ϵ represents a fixed small amount of voltage for increment or decrement [12].
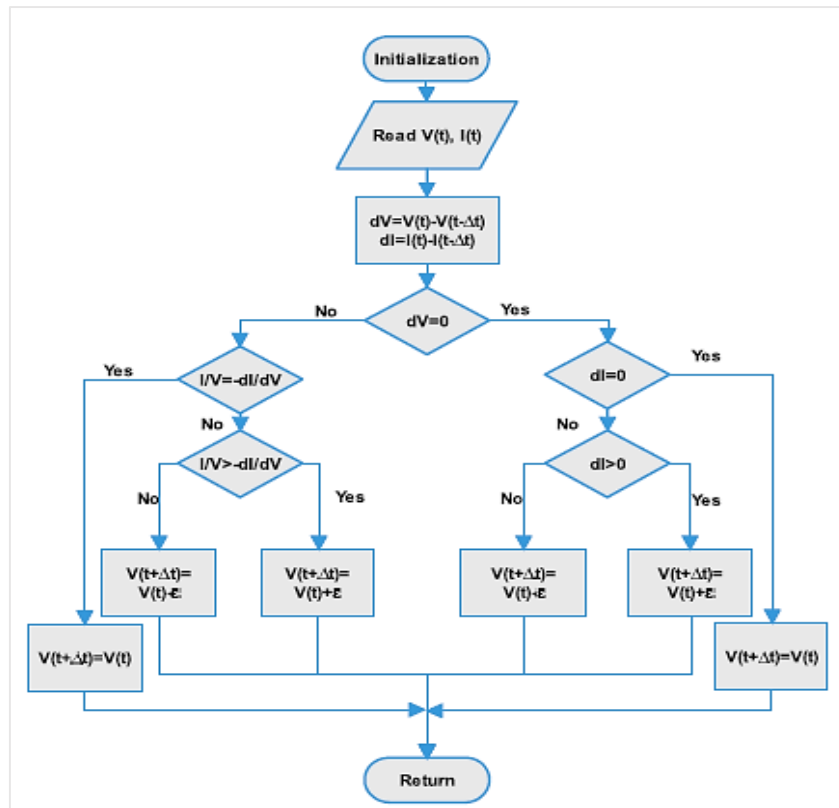
Figure III 4 Flowchart Of The MPPT Algorithm For Incremental Conductance.

III.4. Fuzzy Logic

III.4.1. Introduction

Fuzzy logic is a well-known theory since Zadeh introduced the concept of fuzzy subsets in 1965. Subsequently, in 1974, Mamdani introduced fuzzy control for industrial process regulation, Fuzzy logic has been based on human decision-making and can present good efficiency or acceptable output without knowing a precise mathematical model where the inputs are inaccurate and ambiguous. Fuzzification, rule base, inference engine, and defuzzification are the four major and essential steps in implementing any fuzzy system. In most research conducted so far, the fuzzy toolbox of MATLAB software has been used to design a fuzzy system and create membership functions and rule bases. This will lead to a proper response and will be effective only when there are adequate knowledge and the necessary solar systems expertise. Hence, By utilizing fuzzy logic, the control system can effectively handle the uncertainties and variations inherent in solar energy generation and improve the overall efficiency and performance of the PV system [15].

III.4.2. Fuzzy Logic Generalities

With fuzzy logic, propositions can be represented with degrees of truthfulness and falsehood. For example, the statement today is sunny, might be 100% true if there are no clouds, 80% true if there are a few clouds and 0% true if it rains all day. Mathematical model of system is not required in FLC, hence non linear systems can easily dealt with FLC, It finds applications in control systems, artificial intelligence, and decision analysis, providing a flexible and intuitive approach to modeling and reasoning in situations with inherent fuzziness and uncertainty.

III.4.3. Fuzzy System

Fuzzy systems provide a mechanism to process imprecise inputs who are represented as linguistic variables whiwh are descriptive to the nature of the inputs, and generate appropriate outputs through fuzzy inference using the inputs values and fuzzy rules These fuzzy output sets are then transformed into crisp outputs using defuzzification method that reflect the uncertainty and vagueness of the problem domain. Table (III.1) represent the application of fuzzy logic

Table III 1 Fuzzy Logic Application Domain.

Year	Author	Application
1972 1974 1980 1983 1985 1988 1991	Zadeh. Mamdani & assilian. Fukami et al. Sugeno & Takagi Togar & Watanabe. Dubois & Prade Barrat et al.	• Linguistic approach. • Controlling a steam engine. • Fuzzy conditional inference. • Derivation of fuzzy control rules. • Fuzzy processor. • Approximate reasoning. • Fuzzy oven temperature control.

The general architecture of this fuzzy is represented in this figure:
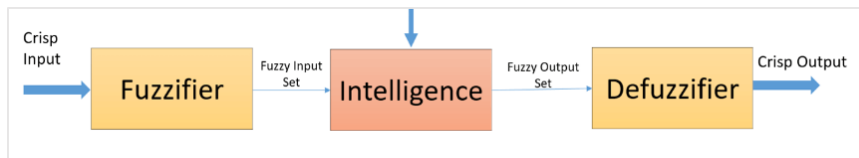
Figure III 5 Fuzzy Architecture.

III.4.4. Fuzzy System Structure

A fuzzy system is composed of four essential parts:

• The knowledge base consists of a data base and a rules base,
• Fuzzy Sets,
• Membership Functions,
• Fuzzy Inference Engine,
• Defuzzification.
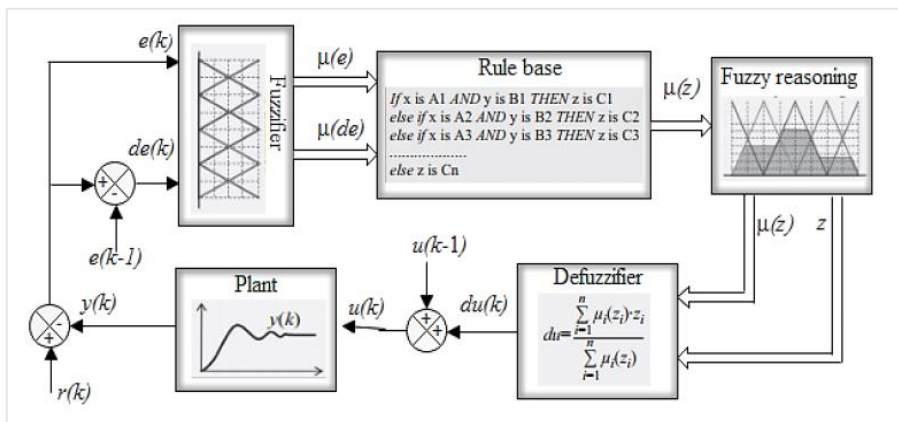
Figure III 6 General Diagram Of a Fuzzy System.

III.5. The Proposed Fuzzy MPPT control Strategie

In many times, the proposed fuzzy MPPT usually depend on the selected linguistic variables. Many of the proposed schemes generally take ΔP, ΔV and/or ΔI or their ratios as inputs, and the change in duty cycle, ΔD as the output. Fuzzy logic controllers generally mimic either the P&O or the Incremental Conductance algorithms. In our work, The proposed fuzzy logic controller based MPPT has two inputs and one output. The two FLC input variables are the error $e(k)$ and change of error $\Delta e(k)$ at sampled times k defined by [16]:

$$e(k) = \frac{P_{pv}(k) - P_{pv}(k-1)}{V_{pv}(k) - V_{pv}(k-1)} \tag{III.4}$$

$$\Delta e(k) = e(k) - e(k-1) \tag{III.5}$$

The figure III.6 and III.7 illustrate the membership functions of the input and output variables employed in this model. These membership functions are represented using triangular functions and comprise five fuzzy sets known as NB (Negative Big), NS (Negative Small), ZE (Zero), PS (Positive Small), and PB (Positive Big)
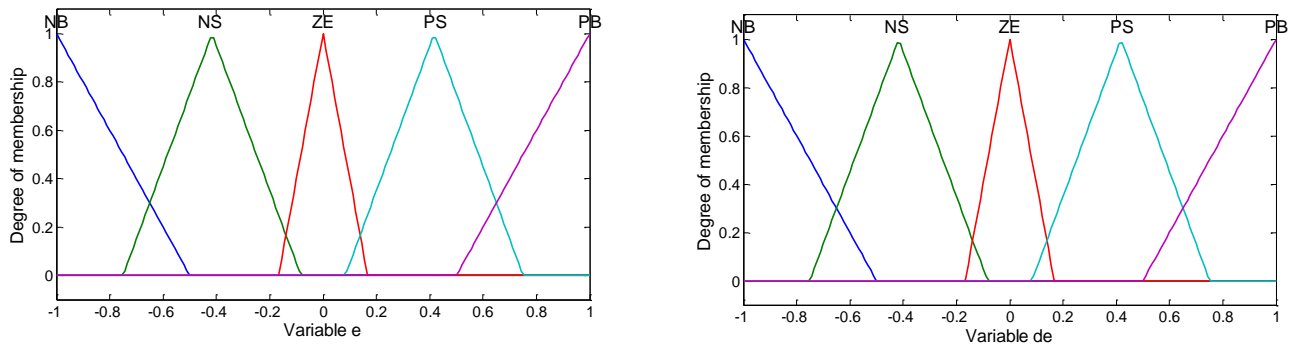
Figure III 7 Inputs Membership Function's.
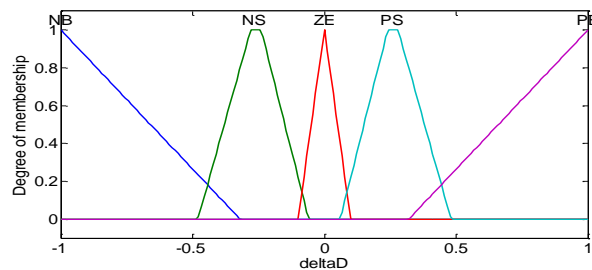
Figure III 8 Output Membership Function.

The fuzzy rule base is a collection of if-then rules where all the necessary information is available for the control parameters. With five membership functions for each input, the fuzzy inference rules of the FLC consist of 25 rules, as illustrated in Table (III.2). These rules are used to determine the controller output for tracking the maximum power point.

The Mamdani method is employed as a fuzzy interface method, utilizing the max-min operation combined with the fuzzy law in this study. The output of the Fuzzy system is defuzzified to calculateΔD.

Table III 2 The rules used to get the output ΔD.

e∆e	NB	NS	ZE	PS	PB
NB	ZE	PB	PB	PB	PB
NS	PB	PS	PS	ZE	ZE
ZE	PS	ZE	ZE	ZE	NS
PS	ZE	ZE	NS	NS	NB
PB	PB	ZE	NS	NB	ZE

III.6 Neural Network Generalities

Recent trends show that AI (ANN) techniques are also used to solve problems of the nonlinear type. Metaheuristics and Neural Networks were found as the most used techniques after surveying the literature. It enables systems to learn, reason, and make decisions, much like humans, by training them with a set of complex instructions. An ANN is a mathematical method that attempts to model the organization of of biological neural network as it seen in Figure (III.9) [18].
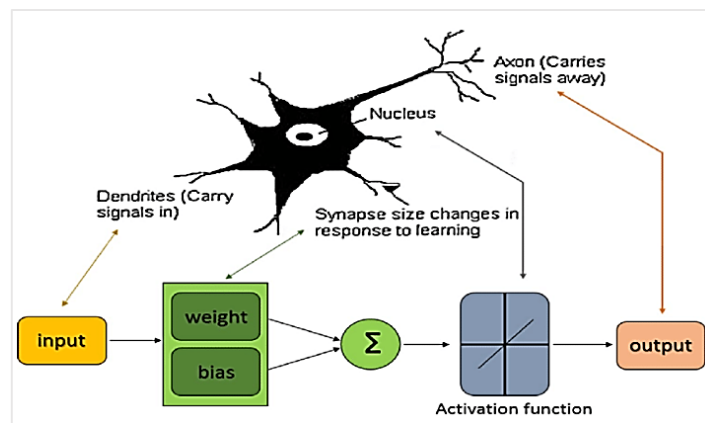
Figure III 9 Common things between the Bioligical Neural and the formel neural.

III.6.1. Neural Network Archetechture

The manual choice of the best ANN architecture to provide the best response for control is tedious. The important parameters of ANN design are the number of hidden layers, the number of neurons in each hidden layer, the type of the activation function and the type of the learning algorithm [16].

There are primarily two types of architectures: looped networks and non-looped networks. Non-looped networks are unidirectional without feedback loops (feed-forward). The output signal is directly obtained after applying the input signal. If not all neurons are output organs, they are referred to as hidden Layers. Looping or feedback networks (recurrent networks) are shown in Figure (III.10).
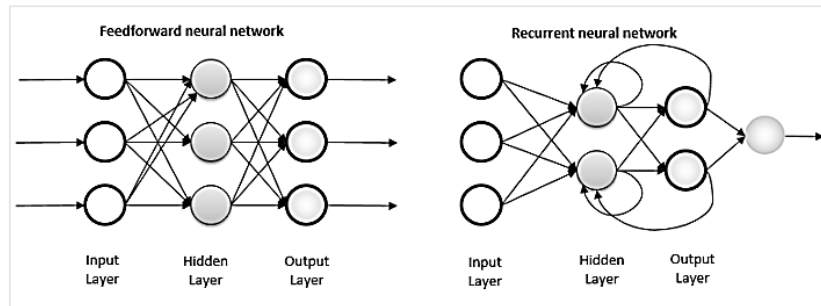
Figure III 10 Artificial Neural Network (ANN) & Reccurent Neural Network.

III.7. The propsed ANN Control for PV system in case of a default

The artificial neural networks (ANNs) have the advantage of accurately replacing complex mathematical models and the ability to imitate some of the brain's process. The ANNs are exploited in the PV systems as it can offer accurate and efective results as the PV system is subjected to various conditions[19].such as if the pv system connected to the grid undergo fault of being an autonom systems its means the grid is isolated in this case The ANN can help enhance the system's response and stability during such fault conditions.So a proposed design of an artificial neural network used for system is presented in Figure (III.11), where the proposed inputs T(time) and Vabc(voltage) The ANN output is the control of breaker, which is utilized to isolate the grid from the PV system and supplying just the load, these are the available data for training the ANN[20].
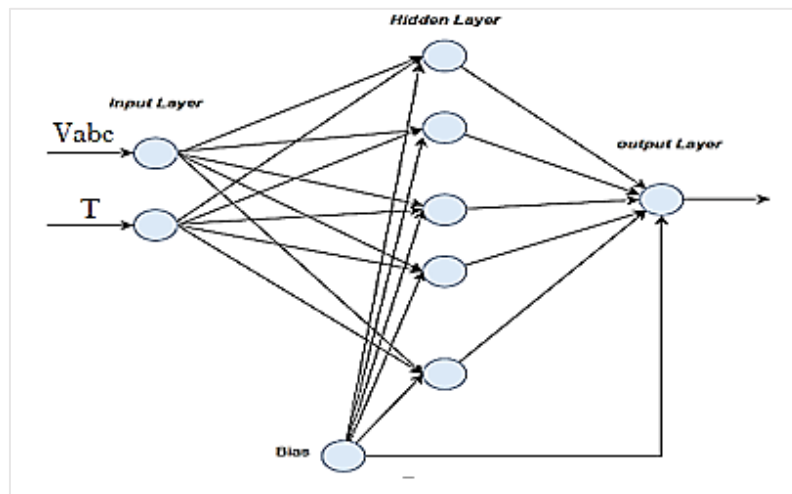
Figure III 11 The peoposed design for Artificial Neural Network used to control the system.

Once a fault is detected, the ANN can make decisions based on pre-trained patterns. It can determine the appropriate response strategy for the PV system, such as disconnecting from the grid and transitioning into standalone mode.

After isolating from the grid, the ANN can provide control signals to adjust the operating parameters of the PV system to ensure stable standalone operation. This may involve regulating power output, maintaining system frequency and voltage within acceptable limits, and managing energy storage systems, if available

Once the fault is resolved, and it is deemed safe to reconnect the PV system, the ANN can facilitate a smooth transition back to grid-connected operation. It can monitor grid conditions, synchronize with the grid, and gradually synchronize the power transfer to avoid any potential disturbances.
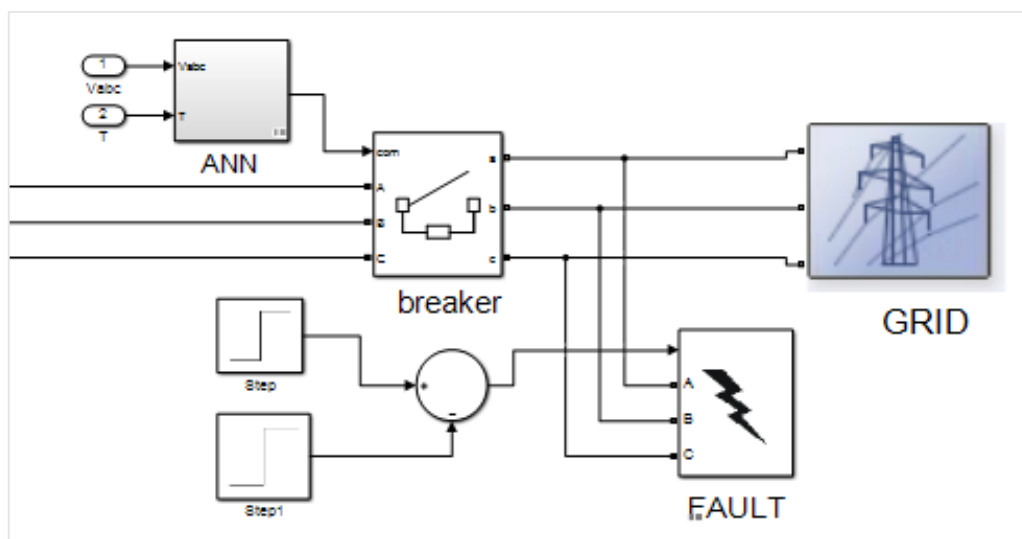
Figure III 12 ANN for system fault**.**

III.8. Conclusion

In conclusion, this chapter provided a comprehensive overview of various key aspects related to power point tracking (PPT) search. It began by introducing the principle of PPT search, followed by a classification of MPPT control techniques into conventional and intelligent approaches. The chapter then delved into the detailed design of specific MPPT techniques, such as P&O, IC, and fuzzy MPPT with different rule tables.

Additionally, it discussed the implementation of intelligent methods, specifically Artificial Neural Networks (ANN), for fault control purposes.

This chapter serves as a valuable resource, equipping readers with knowledge and insights into MPPT search and the diverse range of control intelligent techniques available now.

.

Chapter IV :
Simulation Results

IV.1. Introduction

This chapter is dedicated to a comparative study aimed at evaluating the power behavior of a photovoltaic system. This comparison will be carried out between two control algorithms used to search for the maximum power point in a photovoltaic system. These two algorithms are:

- Perturb and Observe (P&O) algorithm
- Fuzzy logic algorithm, which was theoretically defined in the previous chapter.

Additionally, we will present the simulation of a grid-connected photovoltaic system using both the P&O MPPT (Maximum Power Point Tracking) control and the fuzzy MPPT control. In case of a fault, the storage application and the Artificial Neural Network (ANN) will also be implemented

IV.2. Simulink block of PV system with DC/DC

We simulated the system below under standard conditions (temperature 25°C and irradiance 1000 W/m^2). We took Vpv and Ipv of the PV as inputs to the control block (MPPT) and the duty cycle D as output. Figure (IV.1) shows the Simulink block diagram of the GPV connected to a resistive load via a Boost converter, the DC/DC parameters are given in the Annex.
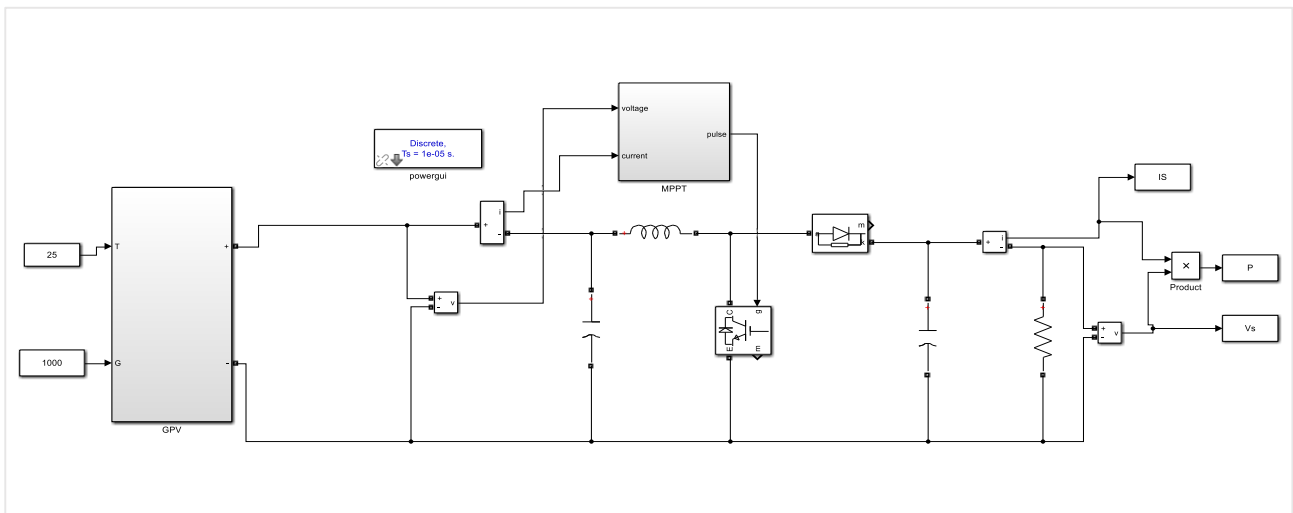
Figure IV 1 GPV Connected With DC/DC Controlled By MPPT (Simulink).

IV.2.1. PV system simulation with P&O algorithm

In this MPPT technique, the duty cycle step size is set to 0.001. The triangular PWM technique is used in the MPPT controller see figure (IV.2) to generate a pulse train to control the state of the Boost switch.
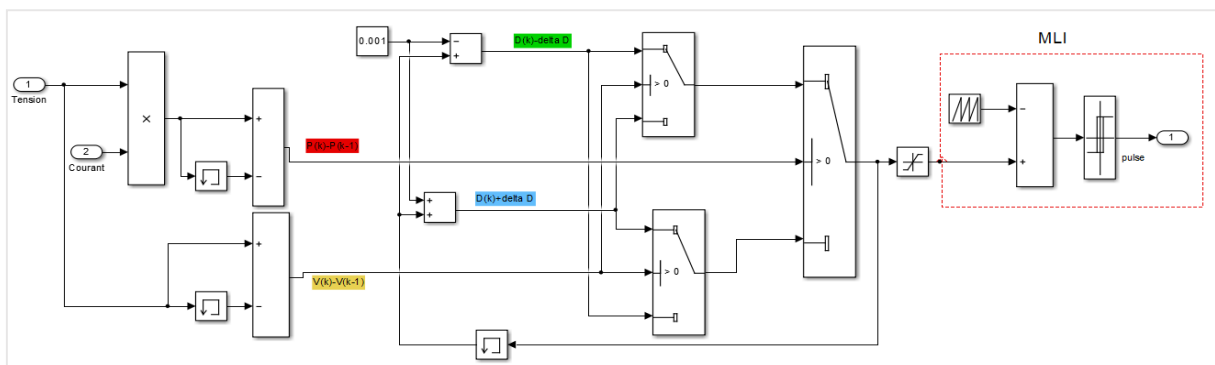
Figure IV 2 P&O Algorithm (Simulink).
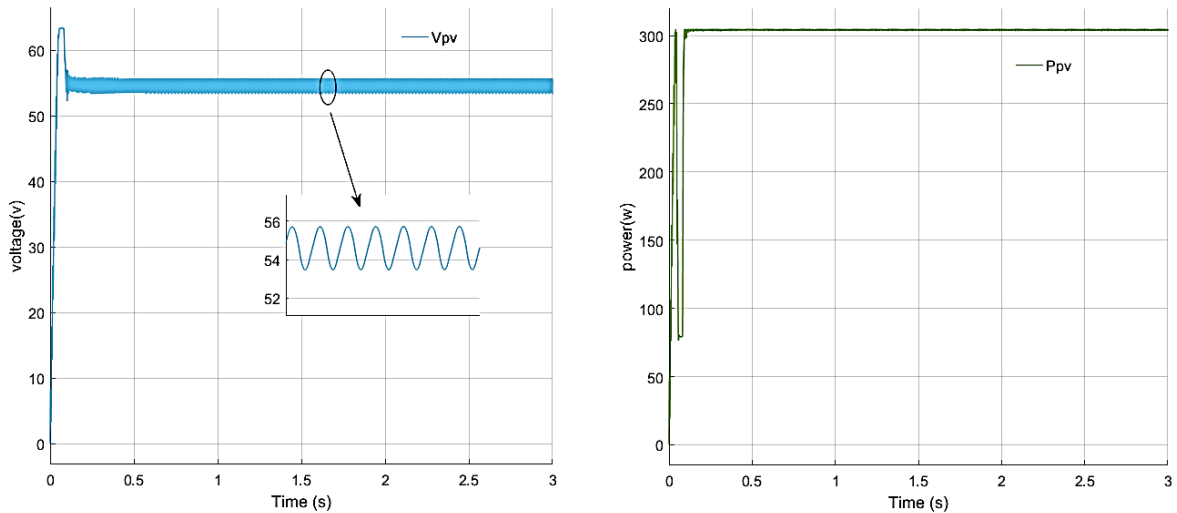
Figure IV 3 GPV 's Output Voltage and power (Vpv&Ppv) with P&O MPPT.
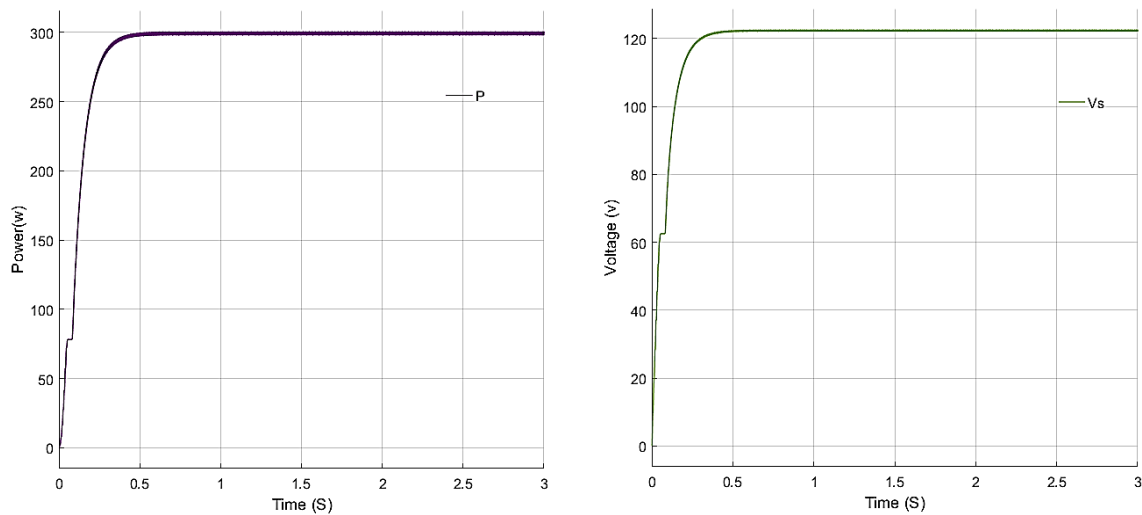
Figure IV 4 DC/DC Output Voltage and power (Vs&P) with P&O MPPT

Figures (IV.3) and show the GPV's output voltage Vpv and power Ppv, respectively. From these two figures, we can observe that the output voltage and power are fluctuating and show ripples.

The output power P of the Boost converter and the voltage Vs across the load of the PV system are shown in figures (IV.4) respectively. The results obtained confirm that the P&O algorithm is capable of tracking the maximum power point as well as transferring the power generated by GPV to the load.

Figure (IV.5) shows a comparison between Ppv power and Boost chopper output power using the P&O algorithm. This figure shows that the P&O algorithm and the Boost converter give better control of the power in the system output.

With the presence of considerable changes and ripples in the GPV output power, the converter effectively improves the variations and shape of this quantity.
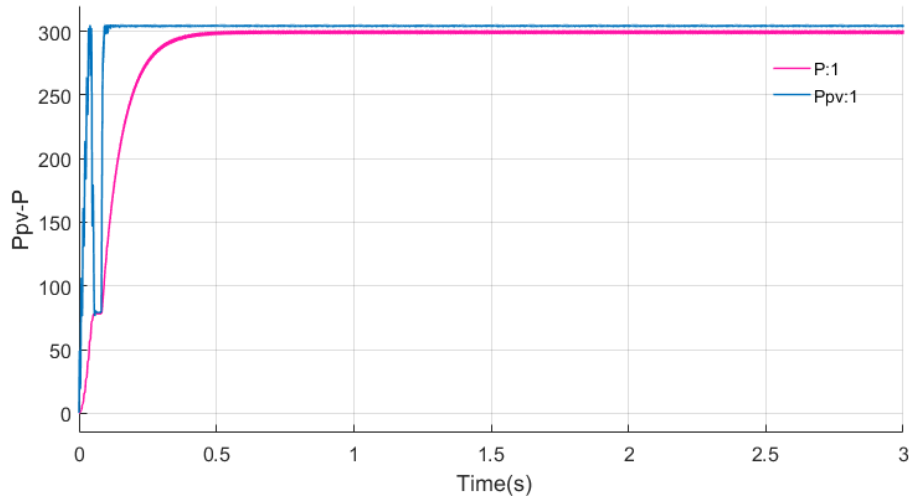
Figure IV 5 comparaison between GPV power and DC/DC output power with P&O MPPT.

IV.2.2. PV system simulation with fuzzy MPPT method
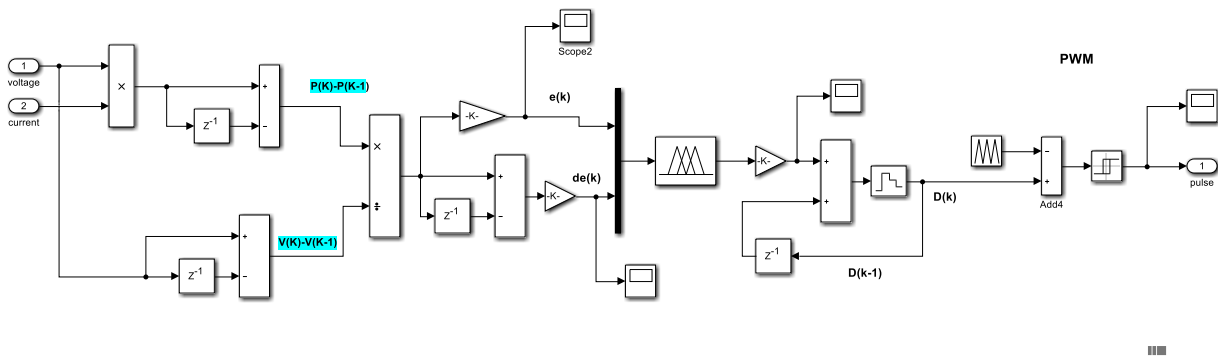
Figure IV 6 The proposed fuzzy MPPT block Simulink.
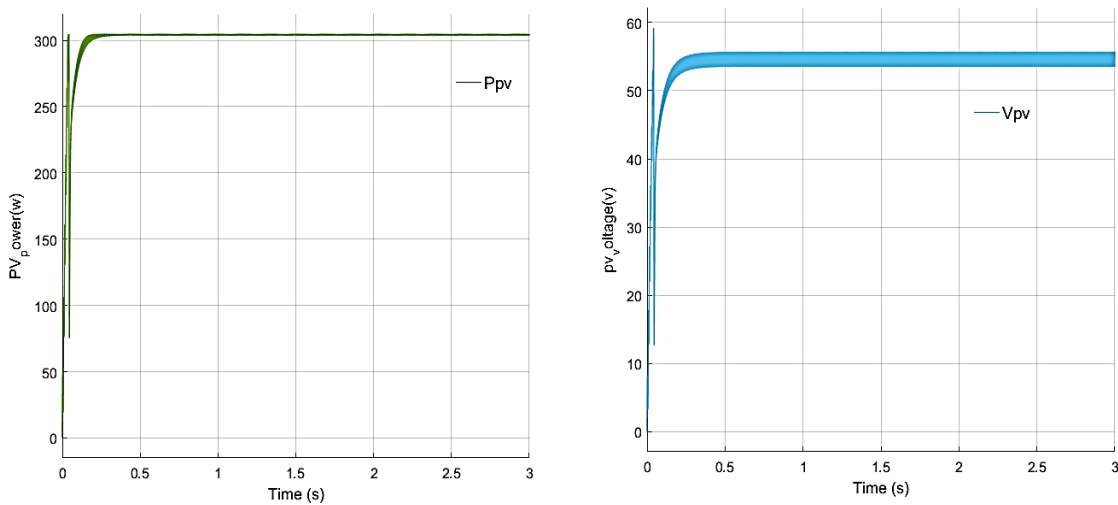
Figure IV 7 GPV 's Output Voltage and power (Vpv&Ppv) with fuzzy MPPT.
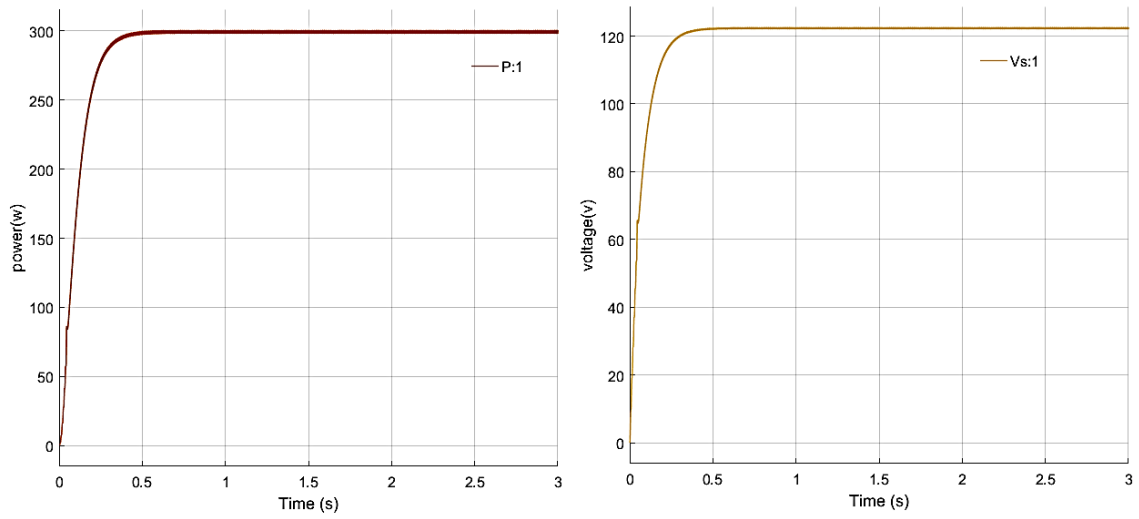
Figure IV 8 DC/DC output's voltage&power with fuzzy MPPT.
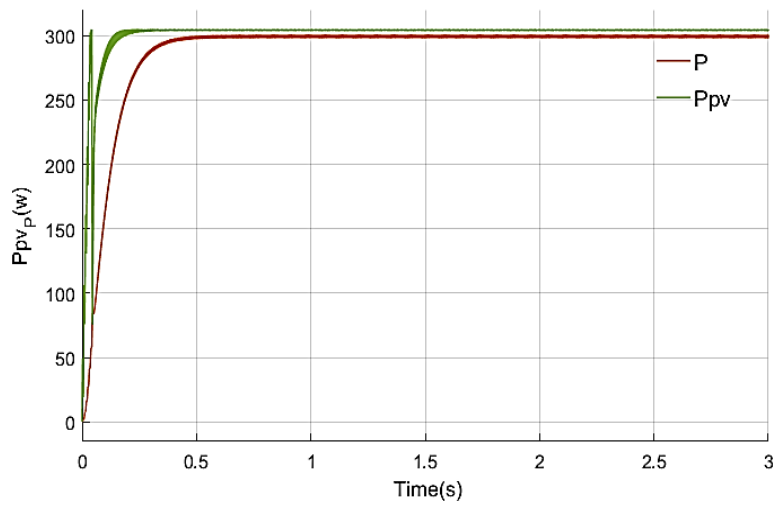
Figure IV 9 comparaison between GPV power and DC/DC output power with fuzzy MPPT.

IV.3. Simulation of the grid-connected photovoltaic system

The figure (IV.10) illustrates the complete structure of the grid-connected photovoltaic generator that we have proposed for study and simulation.
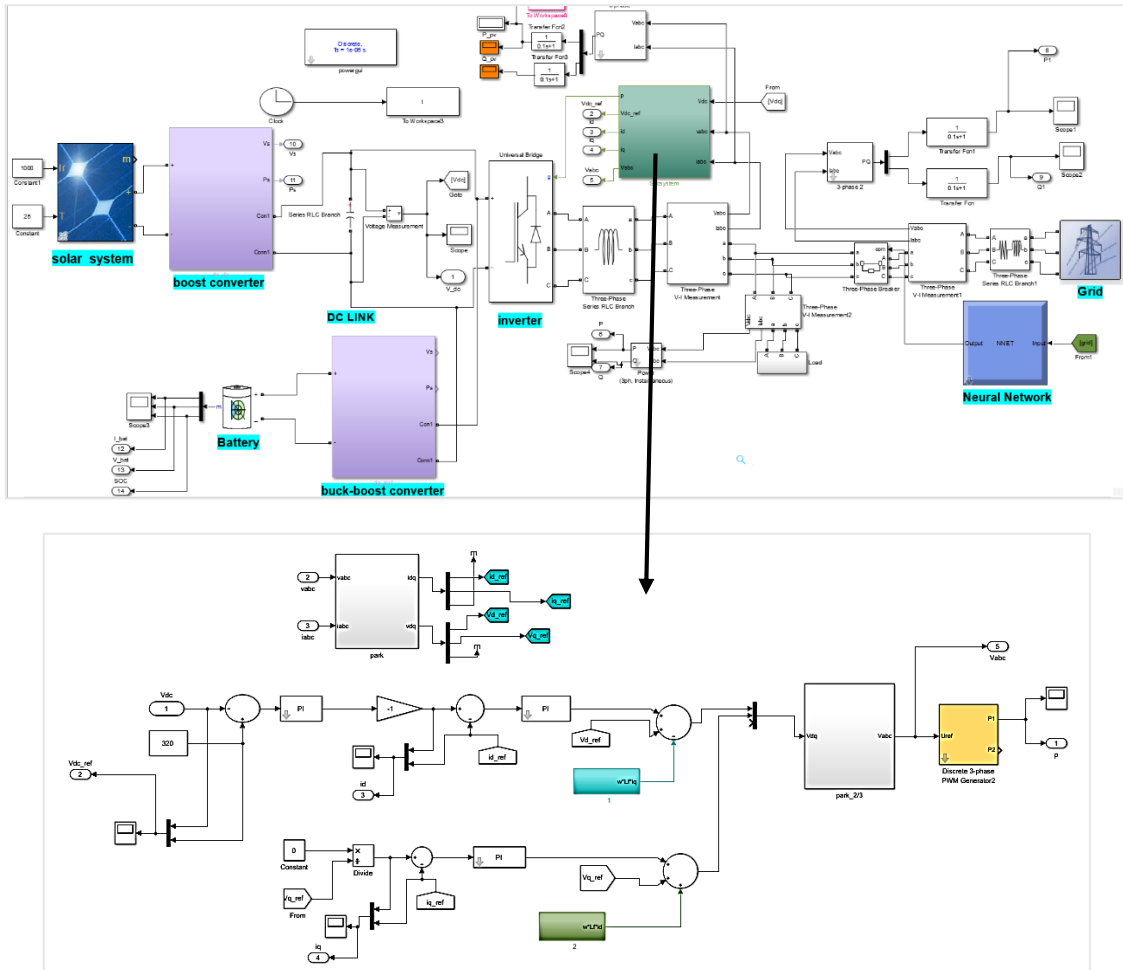
Figure IV 10 Simulink block diagram of the grid-connected photovoltaic system

In a final step, namely the one based on the P&O technique and the fuzzy MPPT, A fault was proposed to the system a scenario of isolating the system from the grid that will affect the PV power with a variation in load power. This profile is illustrated in Figure (IV.11).

The figure represents the waveforms obtained using the P&O technique for the variation of, PV power, voltage, DC bus voltage with reactive power, and the overall power management as per the proposed in the previous chapter. The obtained results confirm the correct operation of power exchanges, according to the PV power state and the power demanded by the load. We also observe the presence of ripples or ondulations in the PV power. The control of the DC bus is assured, and the reactive power is well regulated.

Between the 1s and 2s a fault is applied to the system. The proposed ANN controller has to act on the breaker in order to isolate the grid connection. The system continues working normally with the help of storage system. The ANN controller has the accuaracy and the adaptability of the system to anny fault that could be happen at any time.
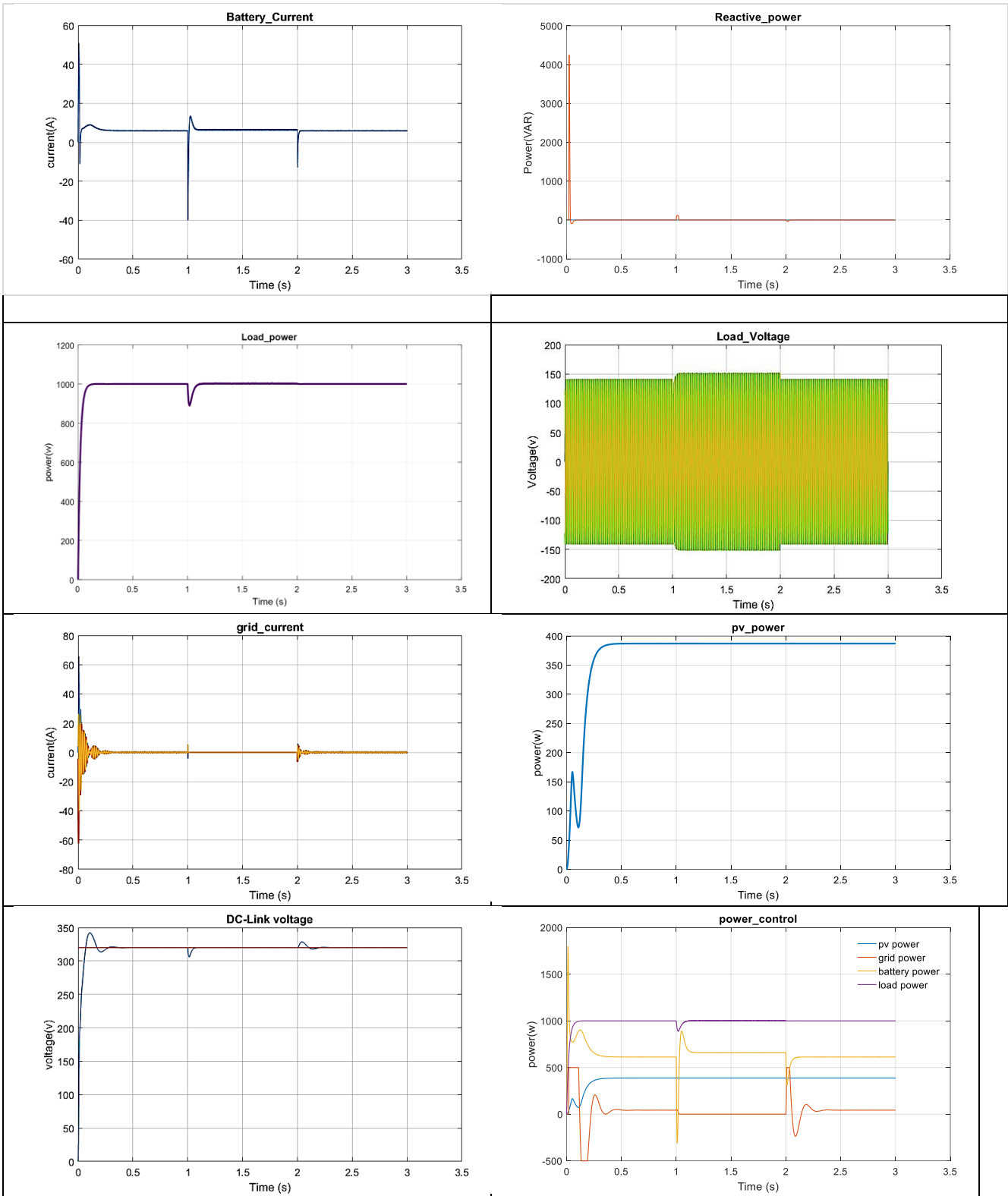
Figure IV 11 Simulation results for GPV connected to the grid- with storage and P&O control.

IV.4 Conclusion

This chapter was concerned with the study of the pv system using conventional control MPPT and comparing it results with the proposed fuzzy control for MPPT, both successfully track the maximum power point, ensuring that the PV system operates at its highest efficiency under varying irradiation conditions.

We moved to the PV connected to the grid that it has his own control so we can create the balance between the power generated by the pv system and the grid according to the load demand, then we disconnected from the grid and transitioning into standalone mode and to achieve that we need to implement the storage and prpose and ANN controller to ensure the sustainability of the system and actually it has proved the efficacity.

General Conclusion

General Conclusion

This study highlights the challenges faced in achieving optimal energy extraction from a photovoltaic (PV) system during varying irradiation conditions. Despite its high energy efficiency, the system exhibited limitations during fluctuations in irradiation. However, the integration of fuzzy logic techniques proved effective in improving dynamic performance, maximizing power extraction, and reducing power fluctuations.

The control of the continuous bus was successfully accomplished using the active and reactive power control, the MPPT technique has been successfully applied in the global system. While the implementation of an intelligent supervisor for energy flow management was not feasible due to time constraints, it remains a valuable avenue for future research.

The simulation results obtained in this study are promising, demonstrating the potential for further investigations. Future research directions may include the development of a fuzzy supervisor for solar energy management and optimization, as well as the exploration of additional intelligent techniques such as neural networks and genetic algorithms. Practical implementation of the proposed algorithms would be crucial for validating their effectiveness in real-world scenarios.

Overall, the study emphasizes the importance of intelligent control strategies in addressing the challenges faced by PV systems. By employing advanced techniques and algorithms, and contributing to a more efficient and sustainable energy landscape

The inclusion of energy storage allows for better management of generated energy, ensuring its optimal utilization. Excess energy can be stored during periods of high generation and utilized during times of low generation or increased demand, thereby enhancing the system's reliability and flexibility.

Artificial intelligence, specifically AI algorithms such as Artificial Neural Networks (ANN), can improve the overall performance of the PV system. By learning from historical data, AI algorithms can make accurate predictions and optimize the operation of the system. This leads to enhanced power generation, improved efficiency, and better adaptability to changing environmental conditions.

The combination of MPPT techniques, energy storage, and artificial intelligence results in a more efficient, reliable, and sustainable grid-connected PV system. It enables optimal utilization of available solar energy, reduces reliance on traditional power sources, and contributes to the overall stability and sustainability of the electrical grid

.

Annex

Annex A

The PV module chosen for our study is the Sunpower E18 305 Solar Panel. It consists of 96 monocrystalline cells and has a maximum power output of 305 W. The module is considered under standard test conditions (STC) with solar irradiance (E) of 1000 W/m2 and a cell temperature (Tc) of 25°C.

For the purpose of modeling, we employed MATLAB as the tool for testing and simulation.

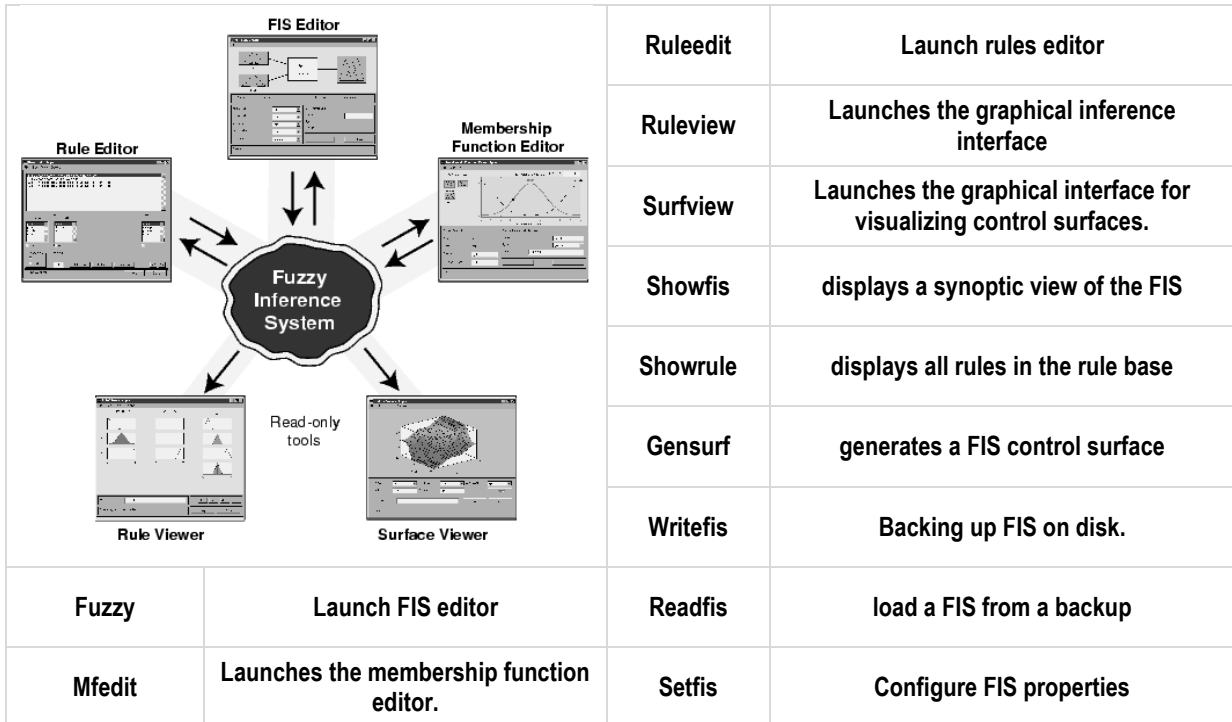| Variables	Values
Maximum power of the module P_{max}	$305w$
Open-circuit voltage V_{co}	$64.2\ V$
Short-Circuit Current I_{cc}	$5.96\ A$
Optimal Voltage V_{mpp}	$54.7\ V$
Optimal Current I_{mpp}	$5.58\ A$
Series resistance R_s	$0.037998\ \Omega$
Shunt Resistance R_{sh}	$993.51\ \Omega$
Number of cells in series N_s	96
Number of parallel cells N_p	1
Short-circuit temperature coefficient K_i	0.0035 A/°C
Open circuit temperature coefficient K_v	-176,6mV / K

DC BOOST converter

We used the following Boost chopper parameters in the Simulink model (Anwesha & Kanhu , 2017):

Parameters	Values
Switching frequency f	1 Khz
Boost chopper input capacityt $C1$	1 mF
Capacity C	3 mF
Inductance L	1.5 mH
Resistance R	50Ω

Annex B

- the main commands used to generate these editors and graphical interfacesCette boite à outils possède 3 éditeurs

FIS Editor the editor for fuzzy inference systems, which is the main editor for defining the number of inputs and outputs, their

		Ruleedit	Launch rules editor
		Ruleview	Launches the graphical inference interface
		Surfview	Launches the graphical interface for visualizing control surfaces.
		Showfis	displays a synoptic view of the FIS
		Showrule	displays all rules in the rule base
		Gensurf	generates a FIS control surface
		Writefis	Backing up FIS on disk.
Fuzzy	Launch FIS editor	Readfis	load a FIS from a backup
Mfedit	Launches the membership function editor.	Setfis	Configure FIS properties

names and type: Mamdani or sugeno

- MembershipFunction Editor: a membership function editor that lets you insert, delete and parameterize membership functions. This is also where you can define the universe of discourse.

- Rule Editor: editor for rules and membership functions, which lets you enter all the rules linking FIS inputs and outputs. You can add, delete or modify a rule, change its connector and/or, even more, modify its weight.

- Rule viewer and surface viewer: graphical interfaces for visualizing inferences directly on the basis of rules, as well as control surfaces. In the rule viewer window, you can check system operation by applying net inputs (numerical values to see how the system works and obtain the net output).

Choice of standardization gains: $K_{e\ initial} = \dfrac{1}{|2 \times e_{max}|}$ et $K_{de\ initial} = \dfrac{1}{|\Delta e_{max}|}$

- After calculating the initial gains, we started tolerating until we achieved the required performance.

Selected tests	K_e	K_{de}	S	Observation
(1)	0.001	0.5	0.5	Lack of precision
(2)	0.0015	0.0001	0.1	Lack of precision
(3)	0.00434	0.33	0.01	Acceptable

Bibliographical References

Bibliography

[1]	B. Fatima, "Modélisation et simulation des sources de production décentralisée Application à l'intégration d'un générateur PV à stockage dans un réseau électrique" , Doctorat Thesis, Abdelhamid Ibn Badis University, Mostaganem, 2018.
[2]	Bernard.M "AN ANALYSIS OF PV SOLAR ELECTRIFICATION ON RURAL LIVELIHOOD TRANSFORMATION",Oslo University, Master Degree, December 2014
[3]	Frederik.K," Assimilation de données satellitaires géostationnaires dans des modèles atmosphériques à aire limitée pour la prévision du rayonnement solaire en région tropicale"doctoral sciences school, technologies, and health ,2019
[4]	BOUALEM,D, "Technique conventionnelles et avancée de poursuite MPPT pour des application photovoltaïque : étude comparative." Ferhat Abbes-Sétif University Magister Thesis, electronique Department TS4/6338, 2007.
[5]	https://www.edfenr.com/lexique/cellule-photovoltaique/ (consulted in 04/18/2023)
[6]	A. Maafi, « A survey on photovoltaic activities in Algeria », *Renewable Energy*, vol. 20, no 1, p. 9-17, mai 2000, doi: 10.1016/S0960-1481(99)00096-8.
[7]	https://mon-panneau-solaire.info/panneaux-solaires/energie-solaire/(consulted 04/20/2023)
[8]	https://www.ef4.be/fr/pv/composants-dun-systeme/systemes-photovoltaiques.html(consulted04/20/2023)
[9]	Richard H, Jr." Solar Forecasting Review" University of CALIFORNIA, SAN DIEGO ,2012
[10]	" Systèmes photovoltaïques ". https://www.ef4.be/fr/pv/composants-dun-systeme/systemes-photovoltaiques.html (seen. 04/23, 2023).
[11]	Cylia.T Ait Ouali.O, "Etude et simulation des techniques MPPT d'un système photovoltaïque ", Final year project,A. MIRA-BEJAIA University,2018/2019
[12]	M.N.Mchalikh and CH.Hmada''Modélisation et simulation d'un système photovoltaïque en fonctionnement autonome et connecté au réseau '' Master Thesis Kasdi Merbah University–Ouargla 2013
[13]	Aicha.A "Application of intelligent control techniques for the control of an integrated PMSG in a wind system".Electrical Engeneering Department Doctorat Thesis Tiaret

Bibliography

[14]	ALBERT, A, "DIAGNOSTIC D'UN SYSTÈME PHOTOVOLTAÏQUE À STOCKAGE PAR ESTIMATION PARAMÉTRIQUE ET COMMANDES ADRC, INTÉGRÉ À UNE CENTRALE AUTONOME DE COGÉNÉRATION D'ÉNERGIE",Doctorat Thesis,Quebec University,2020
[15]	Sabir M, Abd Ghani H and Abd Elhamid L "A New Neural Networks MPPT controller for PV Systems" 1Electrical Engineering Department ,Faculty of Technology, University of M'sila and Electrical Engineering Department High school polytechnic ENP Article 2015
[16]	MAHMOUD N. ALI , KARAR M , MATTI L 2,AND MOHAMED M. F. DARWISH, "An Efficient Fuzzy-Logic Based Variable-Step Incremental Conductance MPPT Method for Grid-Connected PV Systems", Department of Electrical Engineering and Automation, Aalto University, Espoo, Finland, A Review (2021) .
[17]	Fathi M, Jafar Amiri P, "Intelligent MPPT for photovoltaic panels using a novel fuzzy logic and artificial neural networks based on evolutionary algorithms", Article, Department of Biosystems Engineering, Faculty of Agriculture, Bu-Ali Sina University, Hamedan, 6517833131, Iran, 2021
[18]	Yahya. H. "Control and Optimization of an Autonomous Photovoltaic System using Metaheuristic Methods" Doctorat Thesis, Université Mohamed Khider Biskra. Spéciality Electrical engeneering option: automatic 2012
[19]	Mateo Romero, H.F.; González Rebollo, M.A.; Cardeñoso-Payo, V.; Alonso Gómez V.; Redondo Plaza A.; Moyo, R.T.; Hernandez Callejo, L. "Applications of Artificial Intelligence to Photovoltaic Systems:" A Review. Appl. Sci. 2022.
[20]	Ali, M.N.; Mahmoud, K.; Lehtonen, M.; Darwish, M.M.F. Promising MPPT Methods Combining Metaheuristic, Fuzzy-Logic and ANN Techniques for Grid-Connected Photovoltaic. Sensors 2021, 21, 1244.

<div dir="rtl">

ملخص

تتناول هذه الدراسة تطوير وتحسين استراتيجيات التحكم واستخراج الطاقة من الألواح الكهروضوئية (PV)باستخدام تقنيات تحكم مختلفة. تتأثر الطاقة الناتجة للمولد الكهروضوئي (GPV) من خلال عوامل مناخية مختلفة مثل أشعة الشمس ودرجة الحرارة. تم التعامل مع تقنيتين MPPT ، وهما MPPT P&O و MPPTالضبابي. اهتمت الدراسة بحالة الطاقة الكهروضوئية المتصلة بالشبكة. تم تنفيذ طريقتين للتشغيل: الوضع المعزول مع تخزين طاقة البطارية ووضع الاتصال بالشبكة. في هذه الحالة، تم اقتراح وحدة تحكم ذكية تعتمد على الشبكات العصبية الاصطناعية ANN للعمل أثناء وجود الخطأ من أجل ضمان الانتقال إلى الوضع المعزول. تم تطوير اختبارات المحاكاة في بيئة Matlab Simulink. نتائج المحاكاة كانت مشجعة أعطى Fuzzy MPPT أفضل النتائج وتم نشر عملية تحكم ANN بنجاح.

الكلمات الرئيسية: نظام PV ، محول BOOST ، P&O ،MPPT غامض ، ANN.،
</div>

Résumé

Cette étude traite le développement et l'optimisation des stratégies de contrôle et de l'extraction de l'énergie d'un panneau photovoltaïque (PV) en utilisant des techniques de contrôle différentes. La puissance de sortie du générateur photovoltaïque (GPV) est influencée par divers facteurs climatiques tels que l'ensoleillement et la température. Deux techniques de MPPT ont été traitées à savoir la MPPT P&O et la MPPT floue. L'étude a été concernée par le cas d'un PV connecté au réseau. Deux modes de fonctionnement ont été prévus : le mode isolé avec stockage de l'énergie par batterie et le mode connecté au réseau. Dans ce cas un contrôleur intelligent basé sur les réseaux neuronaux artificiels ANN a été proposé pour agir pendant la présence du défaut afin d'assurer le passage en mode isolé. Les essais de simulation ont été développés sous l'environnement Matlab Simulink. Les résultats de simulation sont encourageants. La MPPT floue a donné de meilleurs résultats et le fonctionnement du contrôleur ANN a été implanté avec succès.

Mots-clés : Système PV, convertisseur BOOST, P&O, MPPT floue, ANN.,

Abstract

This study deals with the development and optimization of control strategies and energy extraction from a photovoltaic (PV) panel using different control techniques. The output power of the photovoltaic generator (GPV) is supplied by various climatic factors such as irradiation and temperature. Two MPPT techniques have been treated, namely the P&O MPPT and the fuzzy MPPT. The study was concerned with the case of a PV connected to the network. Two operation modes have been implemented: isolated mode with battery energy storage and grid-connected mode. In this case, an intelligent controller based on ANN artificial neural networks has been proposed to act during the presence of the fault in order to ensure the transition to isolated mode. The simulation tests were developed under the Matlab Simulink environment. Simulation results are encouraged. Fuzzy MPPT gave the best results and ANN controller operation was successfully deployed.

Keywords: PV system, BOOST converter, P&O, fuzzy MPPT, ANN

.